



Measurements of mixed harmonic cumulants in Pb–Pb collisions at $\sqrt{s_{NN}} = 5.02$ TeV

ALICE Collaboration*

ARTICLE INFO

Article history:

Received 8 March 2021

Received in revised form 14 April 2021

Accepted 6 May 2021

Available online 11 May 2021

Editor: M. Doser

ABSTRACT

Correlations between moments of different flow coefficients are measured in Pb–Pb collisions at $\sqrt{s_{NN}} = 5.02$ TeV recorded with the ALICE detector. These new measurements are based on multiparticle mixed harmonic cumulants calculated using charged particles in the pseudorapidity region $|\eta| < 0.8$ with the transverse momentum range $0.2 < p_T < 5.0$ GeV/c. The centrality dependence of correlations between two flow coefficients as well as the correlations between three flow coefficients, both in terms of their second moments, are shown. In addition, a collection of mixed harmonic cumulants involving higher moments of v_2 and v_3 is measured for the first time, where the characteristic signature of negative, positive and negative signs of four-, six- and eight-particle cumulants are observed, respectively. The measurements are compared to the hydrodynamic calculations using iEBE-VISHNU with AMPT and TRENTo initial conditions. It is shown that the measurements carried out using the LHC Run 2 data in 2015 have the precision to explore the details of initial-state fluctuations and probe the nonlinear hydrodynamic response of v_2 and v_3 to their corresponding initial anisotropy coefficients ε_2 and ε_3 . These new studies on correlations between three flow coefficients as well as correlations between higher moments of two different flow coefficients will pave the way to tighten constraints on initial-state models and help to extract precise information on the dynamic evolution of the hot and dense matter created in heavy-ion collisions at the LHC.

© 2021 The Author. Published by Elsevier B.V. This is an open access article under the CC BY license (<http://creativecommons.org/licenses/by/4.0/>). Funded by SCOAP³.

1. Introduction

One of the fundamental questions in the phenomenology of quantum chromodynamics is what are the properties of matter at extreme densities and temperatures where quarks and gluons are in a state of matter called the quark–gluon plasma (QGP) [1,2]. High-energy heavy-ion collisions at the Relativistic Heavy Ion Collider (RHIC) at BNL and the Large Hadron Collider (LHC) at CERN create such a state of strongly interacting matter allowing us to study its properties in the laboratory. Anisotropic flow is a key phenomenon that provides important information about the transport properties of the created QGP matter. Due to large pressure gradients, the anisotropy of the overlapping region between two colliding nuclei causes an anisotropic distribution of the emitted particles in the final state. This anisotropic particle distribution can be quantified by anisotropic flow [3,4] which is characterized by the single-particle azimuthal distribution,

$$P(\varphi) = \frac{1}{2\pi} \left[1 + 2 \sum_{n=1}^{\infty} v_n \cos n(\varphi - \Psi_n) \right]. \quad (1)$$

Here φ is the azimuthal angle of the emitted particle, v_n and Ψ_n are the n -th order flow coefficient and flow symmetry plane, respectively. Both v_n and Ψ_n define the n -th order flow-vector as $\vec{V}_n = v_n e^{in\Psi_n}$. The size and direction of \vec{V}_n related to the initial anisotropy $\vec{\varepsilon}_n$ vector is defined by the moments of the shape of the transverse positions (r, ϕ) of the participating nucleons,

$$\vec{\varepsilon}_n = \varepsilon_n e^{-in\Phi_n} = -\frac{\langle r^n e^{-in\phi} \rangle}{\langle r^n \rangle}, \quad (n > 1) \quad (2)$$

where ε_n and Φ_n are the magnitude and orientation of $\vec{\varepsilon}_n$, respectively, and $\langle \rangle$ stands for the average over all participating nucleons in the initial state. For lower orders, $n = 2$ and 3, originally a linear response of v_n to ε_n was expected, with $v_n = \kappa_n \varepsilon_n$ [5,6] where κ_n is a parameter that encodes the transport properties of the produced QGP. Later on, it was noticed in models that, already in semi-peripheral collisions, the correlation between the initial ε_2 (ε_3) and the final-state v_2 (v_3) is not completely linear, with a non-negligible spread in the correlation between v_n and ε_n [7]. Such a nonlinear response of lower-order v_n should be related to the dynamic evolution of the system, but it was briefly investigated in previous studies [7–9]. For the higher orders, $n \geq 4$, \vec{V}_n receives a significant nonlinear hydrodynamic response from $\vec{\varepsilon}_{2,3}$ in non-central collisions, which was studied in great detail [10–17].

* E-mail address: alice-publications@cern.ch.

One can describe the distribution of final-state anisotropies using a joint probability density function (*p.d.f.*) in terms of v_n and Ψ_n as $P(v_m, v_n, \dots, \Psi_m, \Psi_n, \dots)$. This is sensitive to the spatial anisotropy ε_n , its event-by-event fluctuations, the correlations between different orders of anisotropy coefficients and initial participant planes Φ_n carried by $P(\varepsilon_m, \varepsilon_n, \dots, \Phi_m, \Phi_n, \dots)$ and it also reflects the early state dynamics and the transport properties of the QGP. Although ideally one would like to measure $P(v_m, v_n, \dots, \Psi_m, \Psi_n, \dots)$, this is not straightforward to achieve in experiments, but what can be measured are the projections of the full *p.d.f.* on a finite number of variables [18]. Most of these projected distributions could be classified into the following types: (1) v_n fluctuations $P(v_n)$ for both integrated and differential v_n measurements, (2) Ψ_n fluctuations $P(\Psi_n)$ in different phase space, (3) correlations involving only flow coefficients $P(v_m, v_n, \dots)$, (4) correlations involving only flow symmetry planes $P(\Psi_m, \Psi_n, \dots)$ and (5) mixed correlations carrying both flow coefficients and flow symmetry planes.

The v_n coefficients were measured up to the ninth order with an unprecedented degree of precision [16]. The full *p.d.f.* of single v_n coefficients $P(v_n)$ was either measured with a Bayesian unfolding procedure [19,20] (for $n = 2, 3$ and 4) or constructed via the measured moments (for $n = 2$) [21]. It was found that the $P(v_n)$ distribution, which originates from the *p.d.f.* of initial-state ε_n distribution $P(\varepsilon_n)$, is described better by an elliptic-power function than a Bessel-Gaussian function [21]. It was also realized that during the expansion the produced particles might not share a common flow symmetry plane at different transverse momenta, p_T , and pseudorapidity, η [22,23]. These transverse momentum and pseudorapidity dependent flow vectors fluctuate event-by-event, which also breaks the factorization of two-particle correlations $V(p_T^+, p_T^+)$ into the product of flow coefficients $v_n(p_T^+) \cdot v_n(p_T^+)$ [24–26]. Such phenomena were predicted by hydrodynamic calculations and are found to be sensitive to the initial-state density fluctuations and/or to the specific shear viscosity of the expanding medium [22,23,27]. In addition, analyses of correlations between different order flow vectors [13,28,29] show promise to shed additional light on the initial-state conditions. The correlations between different order symmetry planes were initially investigated in the observable v_{2n/Ψ_n} [30–33]. This was followed by measurements of nonlinear flow modes of higher harmonics by ALICE [14–16,33] as well as event-plane correlations by ATLAS [28].

The correlation observables involving only anisotropic flow coefficients v_m and v_n were at first measured with event-shape engineering studies [13] proceeded by investigations using symmetric cumulants [34], defined as $SC(m, n) = \langle v_n^2 v_m^2 \rangle - \langle v_n^2 \rangle \langle v_m^2 \rangle$. To study such correlations without the dependence on individual flow coefficients, the normalized symmetric cumulant $NSC(m, n)$ was further proposed [29]. It was found that $NSC(3, 2)$, which studies the correlations between v_2^2 and v_3^2 , is very sensitive to the initial conditions and can be used as a good tool to probe initial state ε_2^2 and ε_3^2 correlations. On the other hand, $NSC(4, 2)$ and also NSC involving higher order flow coefficients, are sensitive to both initial conditions and the QGP properties. Thus, these NSC measurements have the potential to distinguish between various models of QGP evolution in hydrodynamic and transport models [9,34–37].

It is evident that the study of correlations between various moments of different flow coefficients will deepen our knowledge of the joint *p.d.f.* for flow magnitudes and angles. However, only correlations involving the second moments of two flow coefficients, v_n^2 and v_m^2 , have been measured utilizing $SC(m, n)$ while the rest have not yet been explored in experiments. In this Letter, an additional step has been made in this direction by using mixed harmonic cumulants (MHC) [38] to investigate correlations involving more than two different flow coefficients and to study

the relationship between higher moments of different flow coefficients in heavy-ion collisions at the LHC. These new measurements establish a milestone for the study of the underlying *p.d.f.* from $P(v_n)$ to $P(v_n, v_m, \dots)$, and significantly improve the overall understanding of the initial conditions and the transport properties of the created QGP at the LHC.

2. Observables and methods

The multiparticle cumulant of mixed harmonics that involves only flow coefficients, named MHC , was introduced in Ref. [38]. It is defined as an m -observable cumulant [39] in terms of azimuthal angles. By construction, lower order correlations have been subtracted to form genuine multiparticle correlations. Thus, MHC is expected to be insensitive to non-flow effects. This was confirmed in the study of MHC using the HIJING model [40], which does not generate collective flow phenomena [38]. For MHC involving only two flow coefficients of second-order, it is identical with the previously defined four-particle symmetric cumulants, i.e. $MHC(v_m^2, v_n^2) = SC(m, n)$. The six-particle cumulant MHC involving v_2^4 and v_3^2 is

$$\begin{aligned} MHC(v_2^4, v_3^2) &= \langle \langle \cos(2\varphi_1 + 2\varphi_2 + 3\varphi_3 - 2\varphi_4 - 2\varphi_5 - 3\varphi_6) \rangle \rangle \\ &\quad - 4 \langle \langle \cos(2\varphi_1 + 3\varphi_2 - 2\varphi_3 - 3\varphi_4) \rangle \rangle \langle \langle \cos(2\varphi_1 - 2\varphi_2) \rangle \rangle \\ &\quad - \langle \langle \cos(2\varphi_1 + 2\varphi_2 - 2\varphi_3 - 2\varphi_4) \rangle \rangle \langle \langle \cos(3\varphi_1 - 3\varphi_2) \rangle \rangle \\ &\quad + 4 \langle \langle \cos(2\varphi_1 - 2\varphi_2) \rangle \rangle^2 \langle \langle \cos(3\varphi_1 - 3\varphi_2) \rangle \rangle. \end{aligned} \quad (3)$$

Here the double angular brackets indicate the averaging procedure performed first over all possible combinations of m -particle tuples that form the m -particle correlation and subsequently the weighted average of all events is calculated with the number of combinations used as an event weight [41]. In the above expressions, lower order (i.e. two- and four-particle) correlations were removed from the six-particle correlation, which results in a genuine six-particle correlation between v_2^4 and v_3^2 . One can rewrite the expression in terms of flow coefficients v_2 and v_3 ,

$$\begin{aligned} MHC(v_2^4, v_3^2) &= \langle v_2^4 v_3^2 \rangle - 4 \langle v_2^2 v_3^2 \rangle \langle v_2^2 \rangle \\ &\quad - \langle v_2^4 \rangle \langle v_3^2 \rangle + 4 \langle v_2^2 \rangle^2 \langle v_3^2 \rangle. \end{aligned} \quad (4)$$

Likewise, one can define other six-particle mixed harmonic cumulants that contain v_2^2 and v_3^2 or v_2^2, v_3^2 and v_4^2 , in terms of flow coefficients,

$$\begin{aligned} MHC(v_2^2, v_3^4) &= \langle v_2^2 v_3^4 \rangle - 4 \langle v_2^2 v_3^2 \rangle \langle v_3^2 \rangle \\ &\quad - \langle v_3^4 \rangle \langle v_2^2 \rangle + 4 \langle v_2^2 \rangle \langle v_3^2 \rangle^2, \end{aligned} \quad (5)$$

$$\begin{aligned} MHC(v_2^2, v_3^2, v_4^2) &= \langle v_2^2 v_3^2 v_4^2 \rangle - \langle v_2^2 v_3^2 \rangle \langle v_4^2 \rangle - \langle v_2^2 v_4^2 \rangle \langle v_3^2 \rangle \\ &\quad - \langle v_3^2 v_4^2 \rangle \langle v_2^2 \rangle + 2 \langle v_2^2 \rangle \langle v_3^2 \rangle \langle v_4^2 \rangle. \end{aligned} \quad (6)$$

Note in general $MHC(v_m^2, v_n^2, v_p^2)$ is different from the so-called higher order symmetric cumulant $SC(m, n, k)$ proposed in [42]. However, $MHC(v_2^2, v_3^2, v_4^2)$ happens to be the same as $SC(2, 3, 4)$.

Similarly, the eight-particle mixed harmonic cumulant is defined as an eight-observable cumulant, which can be written in terms of flow coefficients,

$$\begin{aligned}
MHC(v_2^6, v_3^2) &= \langle v_2^6 v_3^2 \rangle - 9 \langle v_2^4 v_3^2 \rangle \langle v_2^2 \rangle - \langle v_2^6 \rangle \langle v_3^2 \rangle \\
&\quad - 9 \langle v_2^4 \rangle \langle v_2^2 v_3^2 \rangle - 36 \langle v_2^2 \rangle^3 \langle v_3^2 \rangle \\
&\quad + 18 \langle v_2^2 \rangle \langle v_3^2 \rangle \langle v_2^4 \rangle + 36 \langle v_2^2 \rangle^2 \langle v_2^2 v_3^2 \rangle, \quad (7)
\end{aligned}$$

$$\begin{aligned}
MHC(v_2^4, v_3^4) &= \langle v_2^4 v_3^4 \rangle - 4 \langle v_2^4 v_3^2 \rangle \langle v_3^2 \rangle - 4 \langle v_2^2 v_3^4 \rangle \langle v_2^2 \rangle \\
&\quad - \langle v_2^4 \rangle \langle v_3^4 \rangle - 8 \langle v_2^2 v_3^2 \rangle^2 - 24 \langle v_2^2 \rangle^2 \langle v_3^2 \rangle^2 \\
&\quad + 4 \langle v_2^2 \rangle^2 \langle v_3^4 \rangle + 4 \langle v_2^4 \rangle \langle v_3^2 \rangle^2 \\
&\quad + 32 \langle v_2^2 \rangle \langle v_3^2 \rangle \langle v_2^2 v_3^2 \rangle, \quad (8)
\end{aligned}$$

$$\begin{aligned}
MHC(v_2^2, v_3^6) &= \langle v_2^2 v_3^6 \rangle - 9 \langle v_2^2 v_3^4 \rangle \langle v_3^2 \rangle - \langle v_3^6 \rangle \langle v_2^2 \rangle \\
&\quad - 9 \langle v_3^4 \rangle \langle v_2^2 v_3^2 \rangle - 36 \langle v_2^2 \rangle \langle v_3^2 \rangle^3 \\
&\quad + 18 \langle v_2^2 \rangle \langle v_3^2 \rangle \langle v_3^4 \rangle + 36 \langle v_3^2 \rangle^2 \langle v_2^2 v_3^2 \rangle. \quad (9)
\end{aligned}$$

To study genuine multiparticle correlations that are independent of the magnitude of the flow coefficients, the normalized mixed harmonic cumulants $nMHC$ involving two flow coefficients v_m and v_n are constructed according to:

$$nMHC(v_m^k, v_n^l) = \frac{MHC(v_m^k, v_n^l)}{\langle v_m^k \rangle \langle v_n^l \rangle}, \quad (10)$$

Here $m^k \neq n^l$ to ensure that $nMHC(v_m^k, v_n^l)$ does not contain flow symmetry plane correlations. The expression of Eq. (10) is also independent of the magnitudes of v_m and v_n and can therefore be used to quantitatively compare genuine correlations between v_m^k and v_n^l determined from experimental data to those determined from the model calculations. Analogously, for MHC involving three flow coefficients without flow symmetry plane correlations, we define the corresponding $nMHC$,

$$nMHC(v_m^k, v_n^l, v_p^q) = \frac{MHC(v_m^k, v_n^l, v_p^q)}{\langle v_m^k \rangle \langle v_n^l \rangle \langle v_p^q \rangle}. \quad (11)$$

Here $m^k \neq n^l \neq p^q$, and the sum of any two of m^k , n^l and p^q is not equal the third term to avoid flow symmetry plane correlations. Since systematic studies of v_n coefficients were carried out for $n = 1 - 9$ in a previous work [16], this Letter focuses only on the normalized measurements to avoid repeating the earlier discussions on the v_n coefficients themselves. Additionally, multiparticle correlations with sub-event method have been used in the normalizations [14,43], to suppress potential non-flow contamination.

In general, one should be able to construct arbitrary mixed harmonic cumulants to any order. However, due to the limited amount of data available, mixed harmonic cumulants higher than the eighth order will not be examined here. All of the previously mentioned two- and multiparticle azimuthal correlations can be measured by using the latest development of the generic algorithm for multiparticle azimuthal correlations [38].

3. Data sets and systematic uncertainty

This analysis uses data sample from Pb–Pb collisions at $\sqrt{s_{NN}} = 5.02$ TeV recorded with the ALICE detector [44,45] during the LHC Run 2 (year 2015) data-taking period. Minimum bias events were triggered by a coincidence signal in the two scintillator arrays of the V0 detector, VOA and VOC, which cover the pseudorapidity ranges of $2.8 < \eta < 5.1$ and $-3.7 < \eta < -1.7$, respectively [46].

Only events with a reconstructed primary vertex within ± 10 cm from the nominal interaction point along the beam direction were used in this analysis. Removal of background events from, e.g., beam interactions with the residual gas molecules in the beam pipe and pileup events was performed based on the information from the Silicon Pixel Detector (SPD) and the V0 detector. A sample of 55×10^6 Pb–Pb collisions, which passed these event selection criteria, were used for the analysis.

Charged tracks were reconstructed using the Inner Tracking System (ITS) [47] and the Time Projection Chamber (TPC) [48]. The selected tracks are required to have at least 70 TPC space points (out of a maximum of 159), and the average χ^2 per degree of freedom of the track fit to the TPC space points is required to be lower than two. Additionally, a minimum of two hits are required in the ITS to improve the momentum resolution. A selection requiring the pseudorapidity to be within $|\eta| < 0.8$ is applied. Tracks with a transverse momentum $p_T < 0.2$ GeV/c or $p_T > 5.0$ GeV/c were rejected due to the magnetic field and to reduce the contribution from jets, respectively [49]. In addition, a criterion on the maximum distance of closest approach of the track to the collision point of less than 2 cm in the longitudinal direction and less than a p_T -dependent selection in the transverse direction, ranging from 0.2 cm at $p_T = 0.2$ GeV/c to 0.016 cm at $p_T = 5.0$ GeV/c, was applied. This results in a residual contamination from secondary particles from weak decays and from interactions in the detector material of 1–3%, which is negligible in the final systematic uncertainty. These selection criteria result in a transverse momentum dependent efficiency of track reconstruction of about 80%.

Numerous potential sources of systematic uncertainty were investigated in the analysis, including variations of the event and track selection and the uncertainty associated with possible remaining non-flow effects. These are the azimuthal angle correlations not associated with the common flow symmetry planes, including contributions from jets, resonance decays, and are estimated using the HIJING model and found to be negligible for all of the presented observables. The variation of the results with the choice of collision centrality was calculated by alternatively using the SPD to estimate the event multiplicity and was found to contribute less than 5% for all observables. Results with opposite polarities of the magnetic field within the ALICE detector and with narrowing the nominal ± 10 cm range of the reconstructed vertex along the beam direction from the center of the ALICE detector to 9, 8, and 7 cm showed a difference of 0–5.4% compared to results with the default selection criteria. The contribution from pileup events was investigated by varying the selections on the correlations between multiplicities from the V0 and SPD, and was found to be negligible. The sensitivity to the track selection criteria was explored by varying the number of TPC space points and by comparing the results to those obtained with tracks with different requirements on hits in the ITS. The effect of varying the number of TPC space points from 70 to 80 and 90 resulted in a negligible systematic uncertainty. Using different track requirements led to a difference with respect to the default selection criteria of less than 4.3% except for $nMHC(v_2^2, v_3^2, v_4^2)$ where it was about 16%. The systematic uncertainty evaluated for each above-mentioned source found to be statistically significant according to the recommendation in [50] were added in quadrature to obtain the measurements' total systematic uncertainty.

4. Results

The centrality dependence of mixed harmonic cumulants with two and three flow coefficients are measured in Pb–Pb collisions at $\sqrt{s_{NN}} = 5.02$ TeV. The results of $nMHC(v_2^2, v_3^2)$, $nMHC(v_2^2, v_4^2)$, $nMHC(v_3^2, v_4^2)$, and $nMHC(v_2^2, v_3^2, v_4^2)$ are presented in Fig. 1 by blue solid circles, red solid squares, magenta solid stars and green

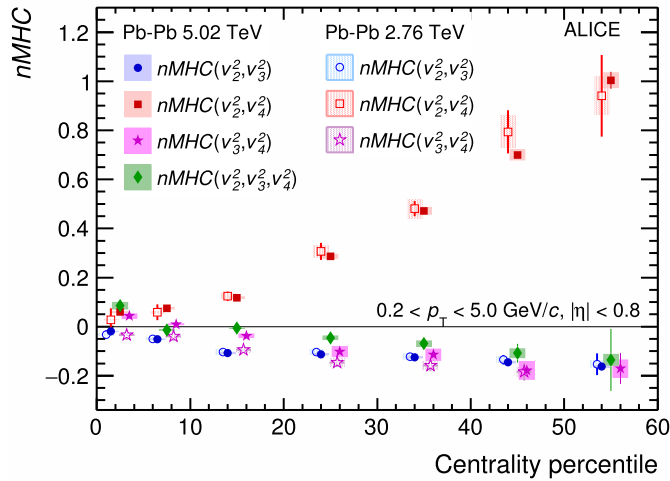


Fig. 1. Centrality dependence of $nMHC(v_2^2, v_3^2)$, $nMHC(v_2^2, v_4^2)$, $nMHC(v_3^2, v_4^2)$ and $nMHC(v_2^2, v_3^2, v_4^2)$ in Pb-Pb collisions at $\sqrt{s_{NN}} = 5.02$ TeV, shown by the solid markers. The statistical (systematic) errors are shown with vertical bars (filled boxes). Comparisons to the previous measurements at 2.76 TeV from Refs. [29,51], shown by the open markers, are also presented. Data points are shifted for visibility.

diamonds, respectively. Positive values of $nMHC(v_2^2, v_4^2)$ and negative values of $nMHC(v_2^2, v_3^2)$ are observed for all centralities, which means that v_2^2 and v_4^2 are correlated while v_2^2 and v_3^2 are anti-correlated. This indicates that finding v_2 larger than $\langle v_2 \rangle$ in an event enhances the probability of finding v_4 larger than $\langle v_4 \rangle$ and v_3 smaller than $\langle v_3 \rangle$ in that event. For $nMHC(v_3^2, v_4^2)$, a similar centrality dependence as for $nMHC(v_2^2, v_3^2)$ is seen for centralities above 20–30% where the nonlinear hydrodynamic response of \vec{V}_4 plays a significant role [14,16]. These new measurements are compared in Fig. 1 to the previously published results at $\sqrt{s_{NN}} = 2.76$ TeV, which were named $SC(m, n)$ in Ref. [29,51], shown with open markers. The results of $nMHC(v_2^2, v_3^2)$, $nMHC(v_2^2, v_4^2)$ are compatible within uncertainties at the two different energies, which indicates a weak dependence on the collision energy of these two observables. However, there are differences for $nMHC(v_3^2, v_4^2)$ between the two studied energies, which increase towards central collisions. In particular, the measurement at 5.02 TeV changes sign from negative to positive in central collisions, while it remains negative at the lower energy. A similar study of multiparticle cumulants in the most central collisions was investigated in great detail in Ref. [52], where a significant effect from centrality fluctuations was found in Pb-Pb collisions at 5.02 TeV. Moreover, the amplitude of the centrality fluctuations depends on how the centrality was determined.

Besides the measurements of correlations between two flow coefficients, the new measurement of correlations between three flow coefficients, $nMHC(v_2^2, v_3^2, v_4^2)$, is shown with green diamonds in Fig. 1. As introduced above, $nMHC(v_2^2, v_3^2, v_4^2)$ is identical to $SC(2, 3, 4)$, which has been recently measured at a lower energy [53]. By construction, the lower order few-particle correlations have been subtracted from the higher order correlations in the $nMHC$. Thus, it is expected that $nMHC(v_2^2, v_3^2, v_4^2)$ should be consistent with zero, if the correlations between three flow coefficients are purely driven by the correlations between two flow coefficients. It is seen in Fig. 1 that the result of $nMHC(v_2^2, v_3^2, v_4^2)$ is located between the $nMHC(v_2^2, v_3^2)$, $nMHC(v_3^2, v_4^2)$ and $nMHC(v_2^2, v_4^2)$ for the centrality classes under study. More specifically, it is positive and closer to $nMHC(v_2^2, v_4^2)$ and $nMHC(v_3^2, v_4^2)$ in the most central collisions, then it changes sign to negative and shows a similar centrality dependence to $nMHC(v_2^2, v_3^2)$ and $nMHC(v_3^2, v_4^2)$ in non-central collisions. The non-zero result of

$nMHC(v_2^2, v_3^2, v_4^2)$ for the presented centrality range shows the existence of genuine correlations between three flow coefficients and thus brings new information toward determining $P(v_n, v_m, \dots)$ that cannot be obtained from measurements of correlations between two flow coefficients.

In order to gain more information on the initial conditions and transport properties of the created QGP at the LHC, the results are compared with those from hydrodynamic model calculations. Results from the hybrid iEBE-VISHNU model with TRENTo initial conditions with specific shear viscosity $\eta/s(T)$ and bulk viscosity $\zeta/s(T)$ extracted from the best fit of a Bayesian analysis [55] as well as calculations with AMPT-initial conditions with $\eta/s = 0.08$ and no bulk viscosity [54] are compared to the data. Both calculations can quantitatively describe the flow coefficients from inclusive and identified hadrons [54,56] and also provide a reasonable description of more complicated flow observables, e.g., nonlinear modes of higher-order flow [15,16]. Besides these two calculations, the iEBE-VISHNU model with AMPT-initial conditions with $\eta/s = 0.20$ and no bulk viscosity is also used. This model does not describe the particle spectra nor the flow coefficients and thus should not be compared with the experimental data. In the remaining text, the hydrodynamic calculations using AMPT initial conditions and $\eta/s = 0.08$ will be referred to as “AMPT calculations”. However, the comparison of hydrodynamic calculation from the same initial state model but with different η/s values can be very useful to study the sensitivity of various $nMHC$ to the η/s of the QGP.

Comparisons of the measured $nMHC(v_2^2, v_3^2)$ and $nMHC(v_2^2, v_4^2)$ to hydrodynamic calculations are shown in Fig. 2. In general, the hydrodynamic calculations with both AMPT and TRENTo initial conditions, shown as blue and red shadowed bands, respectively, predict qualitatively the centrality dependence of $nMHC$. In addition, as v_2 and v_3 are linearly correlated with the initial ε_2 and ε_3 in central and semi-central collisions, compatible results of the final-state $nMHC(v_2^2, v_3^2)$ calculations and the $nMHC(\varepsilon_2^2, \varepsilon_3^2)$ calculations from the initial-state models are expected [38]. This is indeed shown by the shaded areas and the dashed lines in Fig. 2 (left). In the same figure, there is also no difference between the calculations using AMPT-initial conditions with different η/s values. This suggests that for the presented centrality ranges, v_2^2 (v_3^2) is linearly correlated with the initial ε_2^2 (ε_3^2). Thus, the $nMHC(v_2^2, v_3^2)$ measurements shown in Fig. 2 (left) can be used to directly constrain the correlations between the initial anisotropy coefficients ε_2^2 and ε_3^2 without much consideration of the exact value of the transport coefficients in the hydrodynamic models. For $nMHC(v_2^2, v_4^2)$ results shown in Fig. 2 (right), both calculations underestimate the data; the TRENTo calculation fits the data better in central collisions, while the AMPT calculation works slightly better for centralities above 20%. The initial-state calculations of $nMHC(\varepsilon_2^2, \varepsilon_4^2)$ are significantly lower than the final-state $nMHC(v_2^2, v_4^2)$ calculations, which suggests that the correlation between v_2^2 and v_4^2 is not driven solely by the initial correlation between ε_2^2 and ε_4^2 , but it is mainly developed at later stages of the system’s dynamic evolution, especially the nonlinear response contribution to v_4 .

Figure 3 (left) compares hydrodynamic calculations with the $nMHC(v_3^2, v_4^2)$ measurement. In general, both models generate the same trend of centrality dependence as is seen in data. Notably, the AMPT calculations also predict the sign change in central collisions, while the TRENTo calculations remain negative for the entire centrality range. It has also been seen in Ref. [54] that the AMPT calculations always predict a positive correlation in the most central collisions at 2.76 and 5.02 TeV, while the TRENTo calculations are always negative at both collision energies. Although the hydrodynamic calculations of $nMHC(v_3^2, v_4^2)$ from AMPT and TRENTo initial conditions are almost compatible for non-central

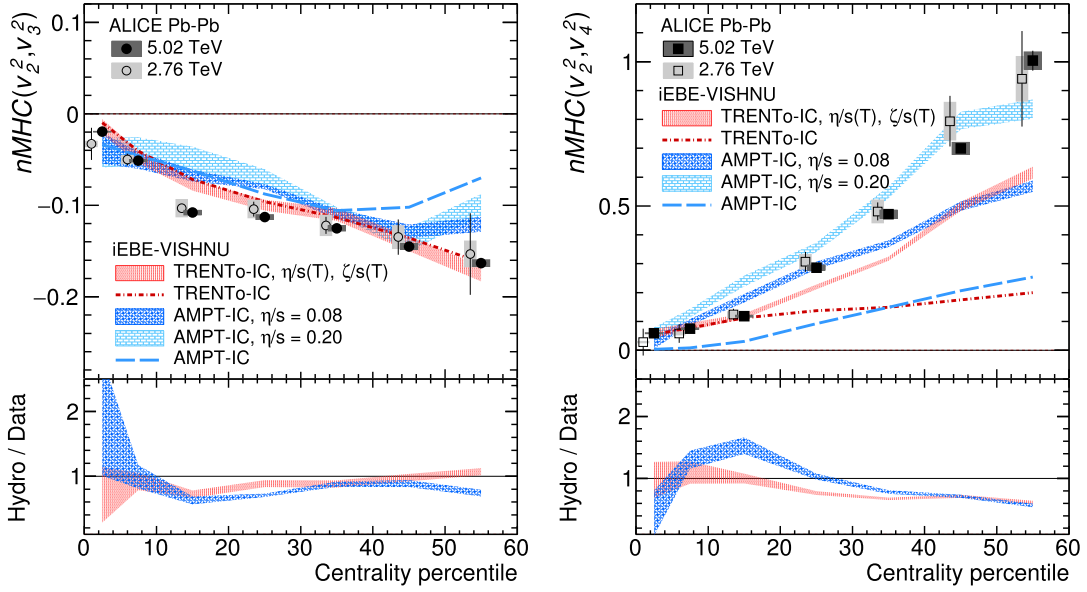


Fig. 2. Centrality dependence of $nMHC(v_2^2, v_3^2)$ and $nMHC(v_2^2, v_4^2)$ in Pb-Pb collisions at $\sqrt{s_{NN}} = 5.02$ TeV (solid markers) and 2.76 TeV (open markers). Statistical uncertainties are shown as vertical bars and systematic uncertainties as filled boxes. The iEBE-VISHNU calculations [54] for Pb-Pb collisions at 5.02 TeV with TRENTo initial conditions (red shaded bands) and AMPT initial conditions (blue shaded bands) are presented, together with the corresponding initial state calculations $nMHC(\varepsilon_2^2, \varepsilon_3^2)$, $nMHC(\varepsilon_2^2, \varepsilon_4^2)$ from the TRENTo (red dot-dash lines) and AMPT model (blue long-dash lines). The same marker (line) styles and colors are used in later figures. Data points are shifted for visibility.

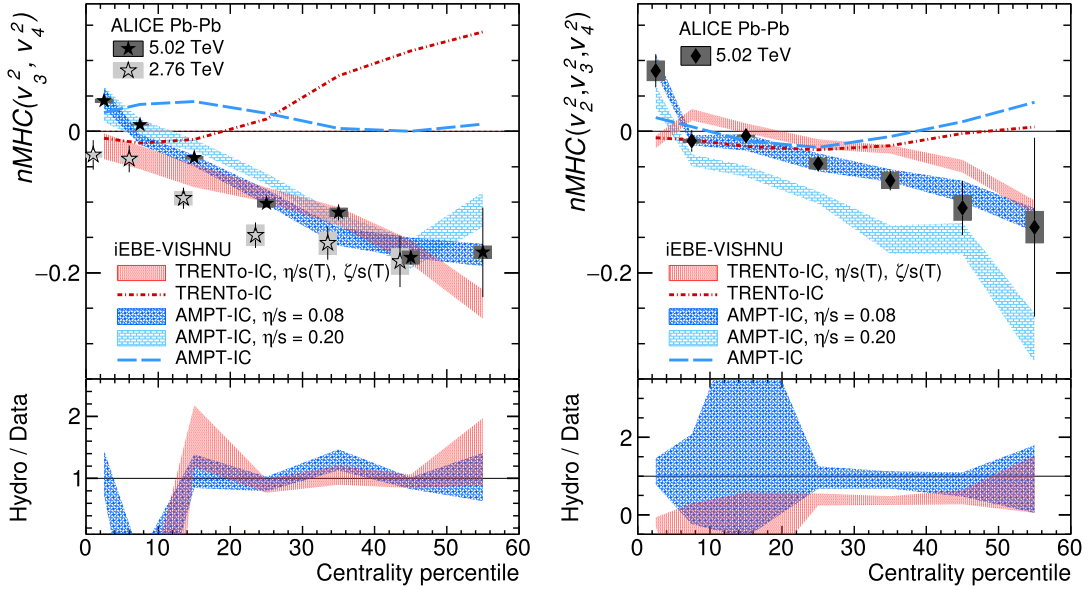


Fig. 3. Centrality dependence of $nMHC(v_3^2, v_4^2)$ and $nMHC(v_2^2, v_3^2, v_4^2)$ in Pb-Pb collisions at $\sqrt{s_{NN}} = 5.02$ TeV (solid markers) and 2.76 TeV (open markers). Statistical uncertainties are shown as vertical bars and systematic uncertainties as filled boxes. Data points are shifted for visibility.

collisions, the initial correlations between ε_3^2 and ε_4^2 , quantified by $nMHC(\varepsilon_3^2, \varepsilon_4^2)$, are utterly different from the two initial-state models, and are far away from the final-state $nMHC(v_3^2, v_4^2)$ calculations. It could be attributed to a significant nonlinear hydrodynamic response in v_4 from ε_2^2 . This nonlinear contribution is strongly anti-correlated with ε_3^2 and plays a dominant role in the final $nMHC(v_3^2, v_4^2)$ results for non-central collisions. On the other hand, in the same centrality region, the linear response of v_4 to ε_4 is rather weak [14], and the contributions from correlations between the initial ε_3^2 and ε_4^2 in the final $nMHC(v_3^2, v_4^2)$ appear to be minor.

To extend the discussion from correlations of two flow coefficients to three flow coefficients, the measurement of $nMHC(v_2^2,$

$v_3^2, v_4^2)$ and its comparison to hydrodynamic calculations with both AMPT and TRENTo initial conditions are presented in Fig. 3 (right). In general, the agreement between the initial $nMHC(\varepsilon_2^2, \varepsilon_3^2, \varepsilon_4^2)$ correlations and the final-state $nMHC(v_2^2, v_3^2, v_4^2)$ calculations worsens as the collision centrality becomes more peripheral, which can be expected due to the increasing contribution from the nonlinear hydrodynamic response in v_4 . Fig. 3 (right) also shows clearly that the calculation with AMPT initial conditions and $\eta/s = 0.08$ describes the data reasonably well. The calculation with $\eta/s = 0.20$ is two times larger than the one with $\eta/s = 0.08$. Such a difference is more significant compared to what has been seen in the correlations between two harmonics, where no obvious difference is observed for $nMHC(v_2^2, v_3^2)$ and $nMHC(v_3^2, v_4^2)$

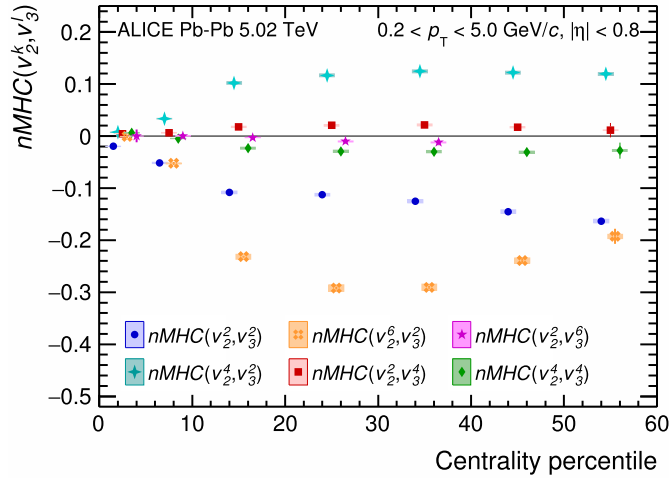


Fig. 4. Centrality dependence of $nMHC$ for Pb-Pb collisions at $\sqrt{s_{NN}} = 5.02$ TeV. Statistical uncertainties are shown as vertical bars and systematic uncertainties as filled boxes. Data points are shifted for visibility.

and only a relatively small difference is seen for $nMHC(v_2^2, v_4^2)$. This demonstrates the novelty of the new correlations between three flow coefficients constraining the transport properties of the QGP. However, despite the fact that the hydrodynamic calculations using TRENTo initial conditions are consistent with the measured $nMHC(v_2^2, v_3^2)$ and $nMHC(v_3^2, v_4^2)$, and also provide a reasonable description of the $nMHC(v_2^2, v_4^2)$ measurement, they significantly underestimate the data by roughly a factor of two. Considering an apparent discrepancy between the data and TRENTo calculations, there is little doubt that the hydrodynamic framework and its corresponding parameters can be better tuned in a future Bayesian analysis if this new $nMHC(v_2^2, v_3^2, v_4^2)$ measurement is used as an input. The first measurement of correlations between three harmonics provides additional independent constraints on the theoretical models beyond those provided by the correlations of two harmonics that have been studied before.

With the recently proposed observable $nMHC$, one can study not only the correlations between two or three different flow coefficients, in terms of their second moments, but also the correlations between the k^{th} order moment of v_m and the l^{th} order moment of v_n where $k \geq 2, l \geq 2$. It is particularly interesting to study the correlations between various moments of v_2 and v_3 because in central and semi-central collisions, both v_2 and v_3 are linearly correlated to their corresponding initial eccentricities ε_2 and ε_3 [8,9]. Thus the measurement of $nMHC(v_2^k, v_3^l)$ in central and semi-central collisions might provide a direct constraint on the initial correlation between $\langle \varepsilon_2^k \rangle$ and $\langle \varepsilon_3^l \rangle$. This information is extremely important for the understanding of the initial conditions of heavy-ion collisions but it has never been measured before. Conversely, the potential nonlinearity of v_2 and v_3 , more pronounced in peripheral collisions, strongly depends on the dynamical evolution of the created QGP. The study of $nMHC(v_2^k, v_3^l)$ will enable a new way to study this effect on v_2 and v_3 .

The first measurements of $nMHC(v_2^k, v_3^l)$ are presented in Fig. 4. In addition to the negative value of $nMHC(v_2^2, v_3^2)$, which has been studied before, positive correlations are observed for both six-particle mixed harmonic cumulants $nMHC(v_2^4, v_3^2)$ and $nMHC(v_2^2, v_3^4)$. The eight-particle mixed harmonic cumulants $nMHC(v_2^6, v_3^2)$, $nMHC(v_2^4, v_3^4)$ and $nMHC(v_2^2, v_3^6)$ are all negative. Such characteristic negative, positive and negative signs of four-, six-, and eight-particle mixed harmonic cumulants, respectively, are very similar to the previously measured pattern for two-, four-, six-, and eight-particle single harmonic cumulants in Pb-Pb collisions [21], which show positive, negative, positive,

and negative signs, respectively. These findings agree qualitatively with the initial-state predictions based on the MC-Glauber [38], AMPT, and TRENTo models [54]. It should be pointed out that the measured negative $nMHC(v_2^2, v_3^2)$ shown above could only confirm the negative correlations of (v_2^2, v_3^2) , while the results presented in Fig. 4 illustrate further the positive correlations of (v_2^4, v_3^2) and (v_2^2, v_3^4) as well as the negative correlations of (v_2^6, v_3^2) , (v_2^4, v_3^4) and (v_2^2, v_3^6) . Moreover, one can see the following hierarchy, $|nMHC(v_2^6, v_3^2)| > |nMHC(v_2^2, v_3^2)| \geq |nMHC(v_2^4, v_3^2)| > |nMHC(v_2^4, v_3^4)| \approx |nMHC(v_2^2, v_3^4)| > |nMHC(v_2^2, v_3^6)|$. This agrees qualitatively with the predictions based on initial-state models [38,54]. Furthermore, the calculations based on the HIJING model [40], which does not generate anisotropic flow in the created system, are consistent with zero [38], and thus do not reproduce the characteristic signs of the multiparticle mixed harmonic cumulants observed in experiments. Future studies with other non-flow models, i.e. PYTHIA [57,58], could confirm if the aforementioned characteristic signs of the multiparticle mixed harmonic cumulants can be regarded as a flow signature and thus could be used for searching for collective flow in small collision systems like pp or pA collisions [59–61].

As mentioned above, for non-peripheral collisions, both v_2 and v_3 are expected to be linearly correlated with the initial eccentricity ε_2 and ε_3 . Thus, the final-state result of $nMHC(v_2^k, v_3^l)$ could reflect the initial correlation between ε_2^k and ε_3^l . This behavior is observed in the case of $nMHC(v_2^2, v_3^2)$, where good agreement with $nMHC(\varepsilon_2^2, \varepsilon_3^2)$ was found. Moving to higher moments of v_2 and/or v_3 , one can further probe the nonlinearity of v_2 (v_3) to ε_2 (ε_3) by seeing if the agreement between the initial and final-state correlations persists, because of the better sensitivity of higher moments to the nonlinear hydrodynamic response. Fig. 5 presents the comparison of data with iEBE-VISHNU calculations with AMPT and TRENTo initial conditions. This figure shows that both calculations describe the measured $nMHC(v_2^4, v_3^2)$ fairly well for central and semi-central collisions. The calculations with AMPT initial conditions work better for more peripheral collisions. At the same time, consistent results are observed between $nMHC(\varepsilon_2^4, \varepsilon_3^2)$ and $nMHC(v_2^4, v_3^2)$, independent of whether the AMPT or TRENTo initial-state model are used. For AMPT calculations, there is no difference between the results using $\eta/s = 0.08$ or 0.20 , which confirms that the precision measurement of $nMHC(v_2^4, v_3^2)$ can offer an additional approach to constrain initial-state models. However, the situation is different in the case of $nMHC(v_2^2, v_3^4)$, shown in Fig. 5 (right). The hydrodynamic calculations with both AMPT and TRENTo initial conditions are compatible with the measurement within the considerable uncertainty, but there is an apparent discrepancy between $nMHC(v_2^2, v_3^4)$ and $nMHC(\varepsilon_2^2, \varepsilon_3^4)$. This does not agree with the naive expectation of both v_2 and v_3 being linearly correlated with their respective initial eccentricities ε_2 and ε_3 , which might be because, generally, the linearity of v_3 to ε_3 is worse than that of v_2 to ε_2 as shown by hydrodynamic calculations [7]. When one examines higher-order moments, the linear response of v_2^4 remains and thus $nMHC(\varepsilon_2^4, \varepsilon_3^2) = nMHC(v_2^4, v_3^2)$ is observed. However, the nonlinearity of v_3^4 becomes non-negligible in non-peripheral collisions, which creates the discrepancy between the initial $nMHC(\varepsilon_2^2, \varepsilon_3^4)$ and final state $nMHC(v_2^2, v_3^4)$ correlations.

This hypothesis is further confirmed in Figs. 6 and 7 where eight-particle cumulants are reported, which involve even higher moments of v_2 and/or v_3 . Firstly, hydrodynamic calculations with AMPT initial conditions quantitatively predict the new measurements of $nMHC(v_2^6, v_3^2)$, $nMHC(v_2^4, v_3^4)$ and $nMHC(v_2^2, v_3^6)$, while the TRENTo calculations show compatible results except for $nMHC(v_2^4, v_3^2)$, where the calculations overestimate the data by a factor of two. Secondly, although in hydrodynamic calculations

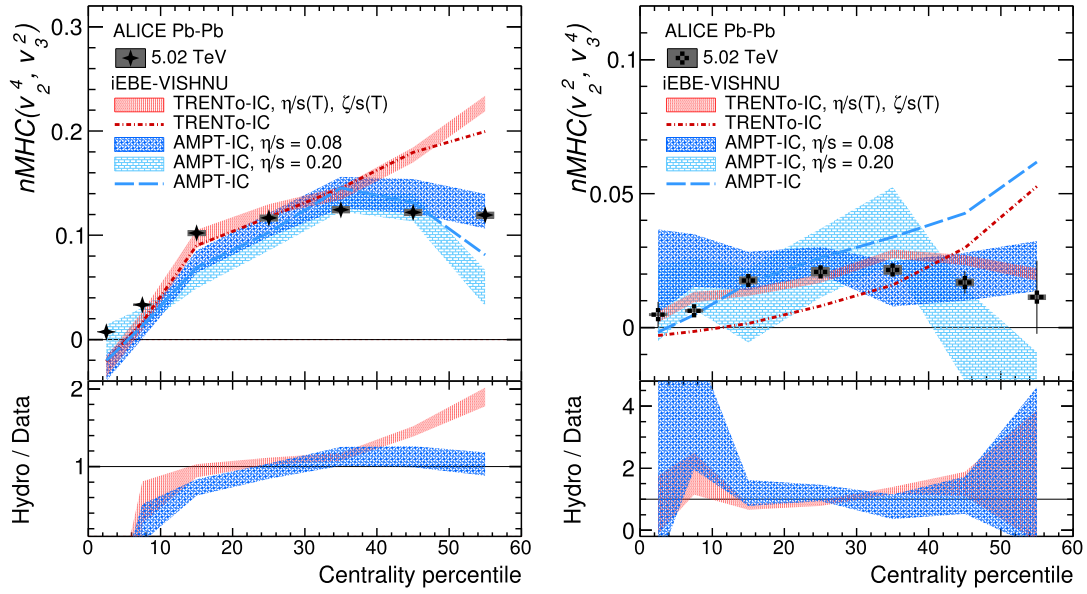


Fig. 5. Centrality dependence of $nMHC(v_2^4, v_3^2)$ and $nMHC(v_2^2, v_3^4)$ in Pb-Pb collision at $\sqrt{s_{NN}} = 5.02$ TeV. Statistical uncertainties are shown as vertical bars and systematic uncertainties as filled boxes.

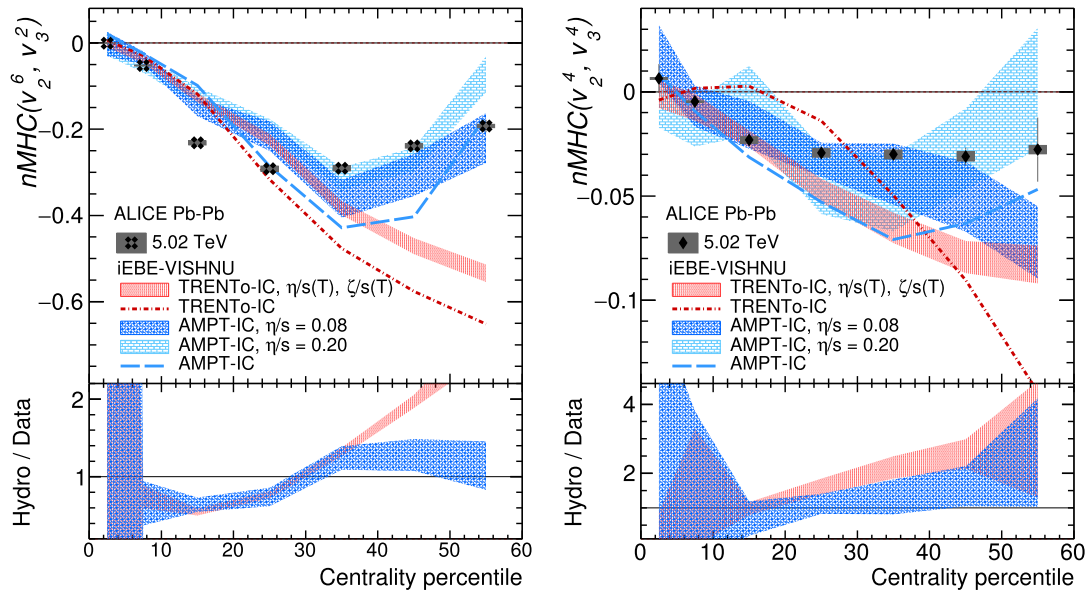


Fig. 6. Centrality dependence of $nMHC(v_2^6, v_3^2)$ (left) and $nMHC(v_2^4, v_3^4)$ (right) in Pb-Pb collisions at $\sqrt{s_{NN}} = 5.02$ TeV. Statistical uncertainties are shown as vertical bars and systematic uncertainties as filled boxes.

with two different initial conditions there is a similar centrality dependence of $nMHC(\varepsilon_2^6, \varepsilon_3^2)$ and $nMHC(v_2^6, v_3^2)$, a clear difference between the two is observed already in semi-central collisions. This difference becomes much larger when fourth and sixth order moments of v_3 are involved, with no obvious agreement between the initial and final-state calculations; this is especially shown by the TRENTo calculations in Figs. 6 (right) and 7. It is expected that the effect of the nonlinearity of v_2 and v_3 will be enhanced when studying $nMHC(v_2^k, v_3^l)$ with higher moments (e.g. $k, l \geq 4$). The resulting $nMHC(v_2^k, v_3^l)$ in the final state, instead of being determined solely by the initial correlations of $nMHC(\varepsilon_2^k, \varepsilon_3^l)$, receive non-negligible contributions from the nonlinearities of higher moments of v_2 and v_3 , developed during the dynamic evolution of the system. Thus, the new measurements of $nMHC(v_2^k, v_3^l)$ presented in this Letter provide direct access to the initial correlations between ε_2^k and ε_3^l when lower moments of v_2 and v_3 are in-

volved, while enabling a new possibility to study the nonlinearities of v_2 and v_3 when higher moments are involved.

5. Summary

The normalized mixed harmonic cumulants $nMHC$ between two and three flow coefficients as well as between higher moments of two flow coefficients, were measured in $\sqrt{s_{NN}} = 5.02$ TeV Pb-Pb collisions with ALICE. It is found that $nMHC(v_2^2, v_4^2)$ is positive, while $nMHC(v_2^2, v_3^2)$ and $nMHC(v_3^2, v_4^2)$ are negative. In addition, the first measurement of three harmonic correlations $nMHC(v_2^2, v_3^2, v_4^2)$ is closer to $nMHC(v_2^2, v_4^2)$ and $nMHC(v_3^2, v_4^2)$ in central collisions, and then becomes closer to $nMHC(v_2^2, v_3^2)$ and $nMHC(v_3^2, v_4^2)$ for more peripheral collisions. These measurements compared with iEBE-VISHNU hydrodynamic calculations using AMPT and TRENTo initial conditions exhibit different sensitiv-

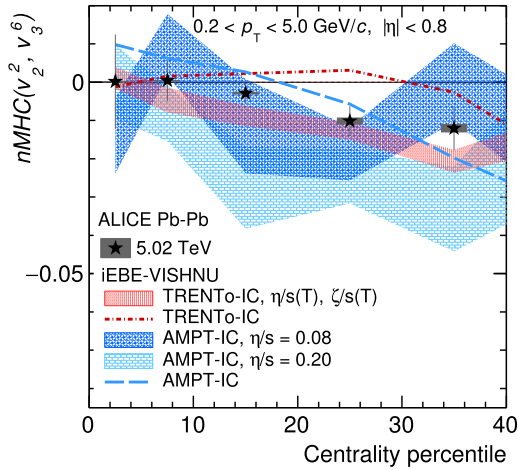


Fig. 7. Centrality dependence of $nMHC(v_2^2, v_3^6)$ in Pb–Pb collisions at $\sqrt{s_{NN}} = 5.02$ TeV. Statistical uncertainties are shown as vertical bars and systematic uncertainties as filled boxes.

ities to the initial conditions and the specific shear viscosity of the QGP. Thus the measurements presented in this Letter can be used to more tightly constrain theoretical models. Furthermore, the correlations between higher moments of v_2 and v_3 were investigated for the first time. The four-, six- and eight-particle mixed cumulants of $nMHC$ show the characteristic signature of negative, positive, and negative signs, respectively, similar to the multiparticle cumulants of single harmonics. The comparison with hydrodynamic calculations reveals that the correlations involving higher-order moments could significantly enhance the contributions that arise from nonlinearities of v_2 and v_3 to the initial eccentricity ε_2 , triangularity ε_3 , respectively. Such contributions mainly develop during the expansion of the system and reflect the time evolution of the shear and bulk viscosities of the QGP. These new measurements of correlations between different moments of two and three flow coefficients, together with comparisons to state-of-the-art hydrodynamic calculations, provide further information on the initial conditions and considerably tighten the constraints on the evolution of the QGP created in heavy-ion collisions at the LHC.

Declaration of competing interest

The authors declare that they have no known competing financial interests or personal relationships that could have appeared to influence the work reported in this paper.

Acknowledgements

The ALICE Collaboration would like to thank all its engineers and technicians for their invaluable contributions to the construction of the experiment and the CERN accelerator teams for the outstanding performance of the LHC complex. The ALICE Collaboration gratefully acknowledges the resources and support provided by all Grid centres and the Worldwide LHC Computing Grid (WLCG) collaboration. The ALICE Collaboration acknowledges the following funding agencies for their support in building and running the ALICE detector: A. I. Alikhanyan National Science Laboratory (Yerevan Physics Institute) Foundation (ANSL), State Committee of Science and World Federation of Scientists (WFS), Armenia; Austrian Academy of Sciences, Austrian Science Fund (FWF): [M 2467-N36] and Nationalstiftung für Forschung, Technologie und Entwicklung, Austria; Ministry of Communications and High Technologies, National Nuclear Research Center, Azerbaijan; Conselho Nacional de Desenvolvimento Científico e Tecnológico (CNPq), Financiadora de Estudos e Projetos (Finep), Fundação de Amparo

à Pesquisa do Estado de São Paulo (FAPESP) and Universidade Federal do Rio Grande do Sul (UFRGS), Brazil; Ministry of Education of China (MOEC), Ministry of Science & Technology of China (NSFC), China; Ministry of Science and Education and Croatian Science Foundation, Croatia; Centro de Aplicaciones Tecnológicas y Desarrollo Nuclear (CEADEN), Cubaenergía, Cuba; Ministry of Education, Youth and Sports of the Czech Republic, Czech Republic; The Danish Council for Independent Research Natural Sciences, the Villum Fonden and Danish National Research Foundation (DNRF), Denmark; Helsinki Institute of Physics (HIP), Finland; Commissariat à l’Énergie Atomique (CEA) and Institut National de Physique Nucléaire et de Physique des Particules (IN2P3) and Centre National de la Recherche Scientifique (CNRS), France; Bundesministerium für Bildung und Forschung (BMBF) and GSI Helmholtzzentrum für Schwerionenforschung GmbH, Germany; General Secretariat for Research and Technology, Ministry of Education, Research and Religions, Greece; National Research, Development and Innovation Office, Hungary; Department of Atomic Energy, Government of India (DAE), Department of Science and Technology, Government of India (DST), University Grants Commission, Government of India (UGC) and Council of Scientific and Industrial Research (CSIR), India; Indonesian Institute of Sciences, Indonesia; Istituto Nazionale di Fisica Nucleare (INFN), Italy; Institute for Innovative Science and Technology, Nagasaki Institute of Applied Science (IIST), Japanese Ministry of Education, Culture, Sports, Science and Technology (MEXT) and Japan Society for the Promotion of Science (JSPS) KAKENHI, Japan; Consejo Nacional de Ciencia (CONACYT) y Tecnología, through Fondo de Cooperación Internacional en Ciencia y Tecnología (FONCICYT) and Dirección General de Asuntos del Personal Académico (DGAPA), Mexico; Nederlandse Organisatie voor Wetenschappelijk Onderzoek (NWO), Netherlands; The Research Council of Norway, Norway; Commission on Science and Technology for Sustainable Development in the South (COMSATS), Pakistan; Pontificia Universidad Católica del Perú, Peru; Ministry of Education and Science, National Science Centre and WUT ID-UB, Poland; Korea Institute of Science and Technology Information and National Research Foundation of Korea (NRF), Republic of Korea; Ministry of Education and Scientific Research, Institute of Atomic Physics and Ministry of Research and Innovation and Institute of Atomic Physics, Romania; Joint Institute for Nuclear Research (JINR), Ministry of Education and Science of the Russian Federation, National Research Centre Kurchatov Institute, Russian Science Foundation and Russian Foundation for Basic Research, Russia; Ministry of Education, Science, Research and Sport of the Slovak Republic, Slovakia; National Research Foundation of South Africa, South Africa; Swedish Research Council (VR) and Knut & Alice Wallenberg Foundation (KAW), Sweden; European Organization for Nuclear Research, Switzerland; Suranaree University of Technology (SUT), National Science and Technology Development Agency (NSDTA) and Office of the Higher Education Commission under NRU project of Thailand, Thailand; Turkish Atomic Energy Agency (TAEK), Turkey; National Academy of Sciences of Ukraine, Ukraine; Science and Technology Facilities Council (STFC), United Kingdom; National Science Foundation of the United States of America (NSF) and United States Department of Energy, Office of Nuclear Physics (DOE NP), United States of America.

References

- [1] T. Lee, Feynman rules of QCD inside a hadron, *Phys. Rev. D* 19 (1979) 1802.
- [2] E.V. Shuryak, Quantum chromodynamics and the theory of superdense matter, *Phys. Rep.* 61 (1980) 71–158.
- [3] J.-Y. Ollitrault, Anisotropy as a signature of transverse collective flow, *Phys. Rev. D* 46 (1992) 229–245.
- [4] S. Voloshin, Y. Zhang, Flow study in relativistic nuclear collisions by Fourier expansion of Azimuthal particle distributions, *Z. Phys. C* 70 (1996) 665–672, [arXiv:hep-ph/9407282](https://arxiv.org/abs/hep-ph/9407282) [hep-ph].

- [5] P.F. Kolb, J. Sollfrank, U.W. Heinz, Anisotropic transverse flow and the quark hadron phase transition, *Phys. Rev. C* 62 (2000) 054909, arXiv:hep-ph/0006129 [hep-ph].
- [6] B. Alver, G. Roland, Collision geometry fluctuations and triangular flow in heavy-ion collisions, *Phys. Rev. C* 81 (2010) 054905, arXiv:1003.0194 [nucl-th], Erratum: *Phys. Rev. C* 82 (2010) 039903.
- [7] H. Niemi, G.S. Denicol, H. Holopainen, P. Huovinen, Event-by-event distributions of azimuthal asymmetries in ultrarelativistic heavy-ion collisions, *Phys. Rev. C* 87 (5) (2013) 054901, arXiv:1212.1008 [nucl-th].
- [8] J. Noronha-Hostler, L. Yan, F.G. Gardim, J.-Y. Ollitrault, Linear and cubic response to the initial eccentricity in heavy-ion collisions, *Phys. Rev. C* 93 (1) (2016) 014909, arXiv:1511.03896 [nucl-th].
- [9] H. Niemi, K.J. Eskola, R. Paatelainen, Event-by-event fluctuations in a perturbative QCD + saturation + hydrodynamics model: determining QCD matter shear viscosity in ultrarelativistic heavy-ion collisions, *Phys. Rev. C* 93 (2) (2016) 024907, arXiv:1505.02677 [hep-ph].
- [10] D. Teaney, L. Yan, Non linearities in the harmonic spectrum of heavy ion collisions with ideal and viscous hydrodynamics, *Phys. Rev. C* 86 (2012) 044908, arXiv:1206.1905 [nucl-th].
- [11] L. Yan, J.-Y. Ollitrault, v_4, v_5, v_6, v_7 : nonlinear hydrodynamic response versus LHC data, *Phys. Lett. B* 744 (2015) 82–87, arXiv:1502.02502 [nucl-th].
- [12] J. Qian, U.W. Heinz, J. Liu, Mode-coupling effects in anisotropic flow in heavy-ion collisions, *Phys. Rev. C* 93 (6) (2016) 064901, arXiv:1602.02813 [nucl-th].
- [13] ATLAS Collaboration, G. Aad, et al., Measurement of the correlation between flow harmonics of different order in lead-lead collisions at $\sqrt{s_{NN}} = 2.76$ TeV with the ATLAS detector, *Phys. Rev. C* 92 (3) (2015) 034903, arXiv:1504.01289 [hep-ex].
- [14] ALICE Collaboration, S. Acharya, et al., Linear and non-linear flow modes in Pb-Pb collisions at $\sqrt{s_{NN}} = 2.76$ TeV, *Phys. Lett. B* 773 (2017) 68–80, arXiv:1705.04377 [nucl-ex].
- [15] ALICE Collaboration, S. Acharya, et al., Non-linear flow modes of identified particles in Pb-Pb collisions at $\sqrt{s_{NN}} = 5.02$ TeV, *J. High Energy Phys.* 06 (2020) 147, arXiv:1912.00740 [nucl-ex].
- [16] ALICE Collaboration, S. Acharya, et al., Linear and non-linear flow modes of charged hadrons in Pb-Pb collisions at $\sqrt{s_{NN}} = 5.02$ TeV, *J. High Energy Phys.* 05 (2020) 085, arXiv:2002.00633 [nucl-ex].
- [17] CMS Collaboration, A.M. Sirunyan, et al., Mixed higher-order anisotropic flow and nonlinear response coefficients of charged particles in PbPb collisions at $\sqrt{s_{NN}} = 2.76$ and 5.02 TeV, *Eur. Phys. J. C* 80 (6) (2020) 534, arXiv:1910.08789 [hep-ex].
- [18] J. Jia, Event-shape fluctuations and flow correlations in ultra-relativistic heavy-ion collisions, *J. Phys. G* 41 (12) (2014) 124003, arXiv:1407.6057 [nucl-ex].
- [19] ATLAS Collaboration, G. Aad, et al., Measurement of the distributions of event-by-event flow harmonics in lead-lead collisions at $\sqrt{s_{NN}} = 2.76$ TeV with the ATLAS detector at the LHC, *J. High Energy Phys.* 11 (2013) 183, arXiv:1305.2942 [hep-ex].
- [20] CMS Collaboration, A.M. Sirunyan, et al., Non-Gaussian elliptic-flow fluctuations in PbPb collisions at $\sqrt{s_{NN}} = 5.02$ TeV, *Phys. Lett. B* 789 (2019) 643–665, arXiv:1711.05594 [nucl-ex].
- [21] ALICE Collaboration, S. Acharya, et al., Energy dependence and fluctuations of anisotropic flow in Pb-Pb collisions at $\sqrt{s_{NN}} = 5.02$ and 2.76 TeV, *J. High Energy Phys.* 07 (2018) 103, arXiv:1804.02944 [nucl-ex].
- [22] U. Heinz, Z. Qiu, C. Shen, Fluctuating flow angles and anisotropic flow measurements, *Phys. Rev. C* 87 (3) (2013) 034913, arXiv:1302.3535 [nucl-th].
- [23] F.G. Gardim, F. Grassi, M. Luzum, J.-Y. Ollitrault, Breaking of factorization of two-particle correlations in hydrodynamics, *Phys. Rev. C* 87 (3) (2013) 031901, arXiv:1211.0989 [nucl-th].
- [24] ALICE Collaboration, S. Acharya, et al., Searches for transverse momentum dependent flow vector fluctuations in Pb-Pb and p-Pb collisions at the LHC, *J. High Energy Phys.* 09 (2017) 032, arXiv:1707.05690 [nucl-ex].
- [25] CMS Collaboration, S. Chatrchyan, et al., Studies of azimuthal dihadron correlations in ultra-central PbPb collisions at $\sqrt{s_{NN}} = 2.76$ TeV, *J. High Energy Phys.* 02 (2014) 088, arXiv:1312.1845 [nucl-ex].
- [26] CMS Collaboration, V. Khachatryan, et al., Evidence for transverse momentum and pseudorapidity dependent event plane fluctuations in PbPb and pPb collisions, *Phys. Rev. C* 92 (3) (2015) 034911, arXiv:1503.01692 [nucl-ex].
- [27] I. Kozlov, M. Luzum, G.S. Denicol, S. Jeon, C. Gale, Signatures of collective behavior in small systems, *Nucl. Phys. A* 931 (2014) 1045–1050, arXiv:1412.3147 [nucl-th].
- [28] ATLAS Collaboration, G. Aad, et al., Measurement of event-plane correlations in $\sqrt{s_{NN}} = 2.76$ TeV lead-lead collisions with the ATLAS detector, *Phys. Rev. C* 90 (2) (2014) 024905, arXiv:1403.0489 [hep-ex].
- [29] ALICE Collaboration, J. Adam, et al., Correlated event-by-event fluctuations of flow harmonics in Pb-Pb collisions at $\sqrt{s_{NN}} = 2.76$ TeV, *Phys. Rev. Lett.* 117 (2016) 182301, arXiv:1604.07663 [nucl-ex].
- [30] FOPI Collaboration, A. Andronic, et al., Transition from in-plane to out-of-plane azimuthal enhancement in Au + Au collisions, *Nucl. Phys. A* 679 (2001) 765–792, arXiv:nucl-ex/0008007.
- [31] E895 Collaboration, P. Chung, et al., Differential elliptic flow in 2-A-GeV - 6-A-GeV Au+Au collisions: a new constraint for the nuclear equation of state, *Phys. Rev. C* 66 (2002) 021901, arXiv:nucl-ex/0112002.
- [32] STAR Collaboration, J. Adams, et al., Azimuthal anisotropy at RHIC: the first and fourth harmonics, *Phys. Rev. Lett.* 92 (2004) 062301, arXiv:nucl-ex/0310029.
- [33] ALICE Collaboration, K. Aamodt, et al., Higher harmonic anisotropic flow measurements of charged particles in Pb-Pb collisions at $\sqrt{s_{NN}} = 2.76$ TeV, *Phys. Rev. Lett.* 107 (2011) 032301, arXiv:1105.3865 [nucl-ex].
- [34] A. Bilandzic, C.H. Christensen, K. Gulbrandsen, A. Hansen, Y. Zhou, Generic framework for anisotropic flow analyses with multiparticle azimuthal correlations, *Phys. Rev. C* 89 (6) (2014) 064904, arXiv:1312.3572 [nucl-ex].
- [35] R.S. Bhalerao, J.-Y. Ollitrault, S. Pal, Characterizing flow fluctuations with moments, *Phys. Lett. B* 742 (2015) 94–98, arXiv:1411.5160 [nucl-th].
- [36] Y. Zhou, K. Xiao, Z. Feng, F. Liu, R. Snellings, Anisotropic distributions in a multiphase transport model, *Phys. Rev. C* 93 (3) (2016) 034909, arXiv:1508.03306 [nucl-ex].
- [37] X. Zhu, Y. Zhou, H. Xu, H. Song, Correlations of flow harmonics in 2.76A TeV Pb-Pb collisions, *Phys. Rev. C* 95 (4) (2017) 044902, arXiv:1608.05305 [nucl-th].
- [38] Z. Moravcova, K. Gulbrandsen, Y. Zhou, Generic algorithm for multi-particle cumulants of azimuthal correlations in high energy nucleus collisions, arXiv:2005.07974 [nucl-th].
- [39] R. Kubo, Generalized cumulant expansion method, *J. Phys. Soc. Jpn.* 17 (1962) 1100–1120.
- [40] M. Gyulassy, X.-N. Wang, HIJING 1.0: a Monte Carlo program for parton and particle production in high-energy hadronic and nuclear collisions, *Comput. Phys. Commun.* 83 (1994) 307, arXiv:nucl-th/9502021 [nucl-th].
- [41] A. Bilandzic, R. Snellings, S. Voloshin, Flow analysis with cumulants: direct calculations, *Phys. Rev. C* 83 (2011) 044913, arXiv:1010.0233 [nucl-ex].
- [42] C. Mordasini, A. Bilandzic, D. Karakoç, S.F. Taghavi, Higher order symmetric cumulants, *Phys. Rev. C* 102 (2) (2020) 024907, arXiv:1901.06968 [nucl-ex].
- [43] P. Huo, K. Gajdosov, J. Jia, Y. Zhou, Importance of non-flow in mixed-harmonic multi-particle correlations in small collision systems, *Phys. Lett. B* 777 (2018) 201–206, arXiv:1710.07567 [nucl-ex].
- [44] ALICE Collaboration, K. Aamodt, et al., The ALICE experiment at the CERN LHC, *J. Instrum.* 3 (2008) S08002.
- [45] ALICE Collaboration, B.B. Abelev, et al., Performance of the ALICE experiment at the CERN LHC, *Int. J. Mod. Phys. A* 29 (2014) 1430044, arXiv:1402.4476 [nucl-ex].
- [46] ALICE Collaboration, E. Abbas, et al., Performance of the ALICE VZERO system, *J. Instrum.* 8 (2013) P10016, arXiv:1306.3130 [nucl-ex].
- [47] ALICE Collaboration, K. Aamodt, et al., Alignment of the ALICE inner tracking system with cosmic-ray tracks, *J. Instrum.* 5 (2010) P03003, arXiv:1001.0502 [physics.ins-det].
- [48] J. Alme, et al., The ALICE TPC, a large 3-dimensional tracking device with fast readout for ultra-high multiplicity events, *Nucl. Instrum. Methods A* 622 (2010) 316–367, arXiv:1001.1950 [physics.ins-det].
- [49] ALICE Collaboration, J. Adam, et al., Anisotropic flow of charged particles in Pb-Pb collisions at $\sqrt{s_{NN}} = 5.02$ TeV, *Phys. Rev. Lett.* 116 (13) (2016) 132302, arXiv:1602.01119 [nucl-ex].
- [50] R. Barlow, Systematic errors: facts and fictions, in: Conference on Advanced Statistical Techniques in Particle Physics, 2002, pp. 134–144, arXiv:hep-ex/0207026.
- [51] ALICE Collaboration, S. Acharya, et al., Systematic studies of correlations between different order flow harmonics in Pb-Pb collisions at $\sqrt{s_{NN}} = 2.76$ TeV, *Phys. Rev. C* 97 (2) (2018) 024906, arXiv:1709.01127 [nucl-ex].
- [52] ATLAS Collaboration, M. Aaboud, et al., Fluctuations of anisotropic flow in Pb+Pb collisions at $\sqrt{s_{NN}} = 5.02$ TeV with the ATLAS detector, *J. High Energy Phys.* 01 (2020) 051, arXiv:1904.04808 [nucl-ex].
- [53] ALICE Collaboration, S. Acharya, et al., Event-by-event multi-harmonic correlations of different flow amplitudes in Pb-Pb collisions at $\sqrt{s_{NN}} = 2.76$ TeV, arXiv:2101.02579 [nucl-ex].
- [54] W. Zhao, H.-j. Xu, H. Song, Collective flow in 2.76 A TeV and 5.02 A TeV Pb+Pb collisions, *Eur. Phys. J. C* 77 (9) (2017) 645, arXiv:1703.10792 [nucl-th].
- [55] J.E. Bernhard, J.S. Moreland, S.A. Bass, Bayesian estimation of the specific shear and bulk viscosity of quark-gluon plasma, *Nat. Phys.* 15 (11) (2019) 1113–1117.
- [56] ALICE Collaboration, S. Acharya, et al., Anisotropic flow of identified particles in Pb-Pb collisions at $\sqrt{s_{NN}} = 5.02$ TeV, *J. High Energy Phys.* 09 (2018) 006, arXiv:1805.04390 [nucl-ex].
- [57] T. Sjöstrand, S. Ask, J.R. Christiansen, R. Corke, N. Desai, P. Ilten, S. Mrenna, S. Prestel, C.O. Rasmussen, P.Z. Skands, An introduction to PYTHIA 8.2, *Comput. Phys. Commun.* 191 (2015) 159–177, arXiv:1410.3012 [hep-ph].
- [58] C. Bierlich, S. Chakraborty, G. Gustafson, L. Lönnblad, Setting the string shoving picture in a new frame, arXiv:2010.07595 [hep-ph].
- [59] C. Loizides, Experimental overview on small collision systems at the LHC, *Nucl. Phys. A* 956 (2016) 200–207, arXiv:1602.09138 [nucl-ex].
- [60] H. Song, Y. Zhou, K. Gajdosova, Collective flow and hydrodynamics in large and small systems at the LHC, *Nucl. Sci. Tech.* 28 (7) (2017) 99, arXiv:1703.00670 [nucl-th].
- [61] J.L. Nagle, W.A. Zajc, Small system collectivity in relativistic hadronic and nuclear collisions, *Annu. Rev. Nucl. Part. Sci.* 68 (2018) 211–235, arXiv:1801.03477 [nucl-ex].

ALICE Collaboration

S. Acharya¹⁴², D. Adamová⁹⁷, A. Adler⁷⁵, J. Adolfsson⁸², G. Aglieri Rinella³⁵, M. Agnello³¹, N. Agrawal⁵⁵, Z. Ahamed¹⁴², S. Ahmad¹⁶, S.U. Ahn⁷⁷, Z. Akbar⁵², A. Akindinov⁹⁴, M. Al-Turany¹⁰⁹, D. Aleksandrov⁹⁰, B. Alessandro⁶⁰, H.M. Alfanda⁷, R. Alfaro Molina⁷², B. Ali¹⁶, Y. Ali¹⁴, A. Alici²⁶, N. Alizadehvandchali¹²⁶, A. Alkin³⁵, J. Alme²¹, T. Alt⁶⁹, L. Altenkamper²¹, I. Altsybeev¹¹⁴, M.N. Anaam⁷, C. Andrei⁴⁹, D. Andreou⁹², A. Andronic¹⁴⁵, V. Anguelov¹⁰⁶, F. Antinori⁵⁸, P. Antonioli⁵⁵, C. Anuj¹⁶, N. Apadula⁸¹, L. Aphecetche¹¹⁶, H. Appelshäuser⁶⁹, S. Arcelli²⁶, R. Arnaldi⁶⁰, I.C. Arsene²⁰, M. Arslanok^{147,106}, A. Augustinus³⁵, R. Averbeck¹⁰⁹, S. Aziz⁷⁹, M.D. Azmi¹⁶, A. Badalà⁵⁷, Y.W. Baek⁴², X. Bai¹⁰⁹, R. Bailhache⁶⁹, Y. Bailung⁵¹, R. Bala¹⁰³, A. Balbino³¹, A. Baldisseri¹³⁹, M. Ball⁴⁴, D. Banerjee⁴, R. Barbera²⁷, L. Barioglio^{107,25}, M. Barlou⁸⁶, G.G. Barnaföldi¹⁴⁶, L.S. Barnby⁹⁶, V. Barret¹³⁶, C. Bartels¹²⁹, K. Barth³⁵, E. Bartsch⁶⁹, F. Baruffaldi²⁸, N. Bastid¹³⁶, S. Basu^{82,144}, G. Batigne¹¹⁶, B. Batyunya⁷⁶, D. Bauri⁵⁰, J.L. Bazo Alba¹¹³, I.G. Bearden⁹¹, C. Beattie¹⁴⁷, I. Belikov¹³⁸, A.D.C. Bell Hechavarria¹⁴⁵, F. Bellini³⁵, R. Bellwied¹²⁶, S. Belokurova¹¹⁴, V. Belyaev⁹⁵, G. Bencedi^{70,146}, S. Beole²⁵, A. Bercuci⁴⁹, Y. Berdnikov¹⁰⁰, A. Berdnikova¹⁰⁶, D. Berenyi¹⁴⁶, L. Bergmann¹⁰⁶, M.G. Besoiu⁶⁸, L. Betev³⁵, P.P. Bhaduri¹⁴², A. Bhasin¹⁰³, I.R. Bhat¹⁰³, M.A. Bhat⁴, B. Bhattacharjee⁴³, P. Bhattacharya²³, L. Bianchi²⁵, N. Bianchi⁵³, J. Bielčik³⁸, J. Bielčíková⁹⁷, J. Biernat¹¹⁹, A. Bilandzic¹⁰⁷, G. Biro¹⁴⁶, S. Biswas⁴, J.T. Blair¹²⁰, D. Blau⁹⁰, M.B. Blidaru¹⁰⁹, C. Blume⁶⁹, G. Boca²⁹, F. Bock⁹⁸, A. Bogdanov⁹⁵, S. Boi²³, J. Bok⁶², L. Boldizsár¹⁴⁶, A. Bolozdynya⁹⁵, M. Bombara³⁹, P.M. Bond³⁵, G. Bonomi¹⁴¹, H. Borel¹³⁹, A. Borissov⁸³, H. Bossi¹⁴⁷, E. Botta²⁵, L. Bratrud⁶⁹, P. Braun-Munzinger¹⁰⁹, M. Bregant¹²², M. Broz³⁸, G.E. Bruno^{108,34}, M.D. Buckland¹²⁹, D. Budnikov¹¹⁰, H. Buesching⁶⁹, S. Bufalino³¹, O. Bugnon¹¹⁶, P. Buhler¹¹⁵, Z. Buthelezi^{73,133}, J.B. Butt¹⁴, S.A. Bysiak¹¹⁹, D. Caffarri⁹², M. Cai^{28,7}, A. Caliva¹⁰⁹, E. Calvo Villar¹¹³, J.M.M. Camacho¹²¹, R.S. Camacho⁴⁶, P. Camerini²⁴, F.D.M. Canedo¹²², A.A. Capon¹¹⁵, F. Carnesecchi²⁶, R. Caron¹³⁹, J. Castillo Castellanos¹³⁹, E.A.R. Casula²³, F. Catalano³¹, C. Ceballos Sanchez⁷⁶, P. Chakraborty⁵⁰, S. Chandra¹⁴², W. Chang⁷, S. Chapeland³⁵, M. Chartier¹²⁹, S. Chattopadhyay¹⁴², S. Chattopadhyay¹¹¹, A. Chauvin²³, T.G. Chavez⁴⁶, C. Cheshkov¹³⁷, B. Cheynis¹³⁷, V. Chibante Barroso³⁵, D.D. Chinellato¹²³, S. Cho⁶², P. Chochula³⁵, P. Christakoglou⁹², C.H. Christensen⁹¹, P. Christiansen⁸², T. Chujo¹³⁵, C. Cicalo⁵⁶, L. Cifarelli²⁶, F. Cindolo⁵⁵, M.R. Ciupek¹⁰⁹, G. Clai^{55,II}, J. Cleymans¹²⁵, F. Colamaria⁵⁴, J.S. Colburn¹¹², D. Colella^{108,54,34,146}, A. Collu⁸¹, M. Colocci^{35,26}, M. Concas^{60,III}, G. Conesa Balbastre⁸⁰, Z. Conesa del Valle⁷⁹, G. Contin²⁴, J.G. Contreras³⁸, T.M. Cormier⁹⁸, P. Cortese³², M.R. Cosentino¹²⁴, F. Costa³⁵, S. Costanza²⁹, P. Crochet¹³⁶, E. Cuautle⁷⁰, P. Cui⁷, L. Cunqueiro⁹⁸, A. Dainese⁵⁸, F.P.A. Damas^{116,139}, M.C. Danisch¹⁰⁶, A. Danu⁶⁸, I. Das¹¹¹, P. Das⁸⁸, P. Das⁴, S. Das⁴, S. Dash⁵⁰, S. De⁸⁸, A. De Caro³⁰, G. de Cataldo⁵⁴, L. De Cilladi²⁵, J. de Cuveland⁴⁰, A. De Falco²³, D. De Gruttola³⁰, N. De Marco⁶⁰, C. De Martin²⁴, S. De Pasquale³⁰, S. Deb⁵¹, H.F. Degenhardt¹²², K.R. Deja¹⁴³, L. Dello Stritto³⁰, S. Delsanto²⁵, W. Deng⁷, P. Dhankher¹⁹, D. Di Bari³⁴, A. Di Mauro³⁵, R.A. Diaz⁸, T. Dietel¹²⁵, Y. Ding⁷, R. Divià³⁵, D.U. Dixit¹⁹, Ø. Djuvsland²¹, U. Dmitrieva⁶⁴, J. Do⁶², A. Dobrin⁶⁸, B. Dönigus⁶⁹, O. Dordic²⁰, A.K. Dubey¹⁴², A. Dubla^{109,92}, S. Dudi¹⁰², M. Dukhishyam⁸⁸, P. Dupieux¹³⁶, T.M. Eder¹⁴⁵, R.J. Ehlers⁹⁸, V.N. Eikeland²¹, D. Elia⁵⁴, B. Erazmus¹¹⁶, F. Ercolessi²⁶, F. Erhardt¹⁰¹, A. Erokhin¹¹⁴, M.R. Ersdal²¹, B. Espagnon⁷⁹, G. Eulisse³⁵, D. Evans¹¹², S. Evdokimov⁹³, L. Fabbietti¹⁰⁷, M. Faggin²⁸, J. Faivre⁸⁰, F. Fan⁷, A. Fantoni⁵³, M. Fasel⁹⁸, P. Fecchio³¹, A. Feliciello⁶⁰, G. Feofilov¹¹⁴, A. Fernández Téllez⁴⁶, A. Ferrero¹³⁹, A. Ferretti²⁵, V.J.G. Feuillard¹⁰⁶, J. Figiel¹¹⁹, S. Filchagin¹¹⁰, D. Finogeev⁶⁴, F.M. Fionda²¹, G. Fiorenza⁵⁴, F. Flor¹²⁶, A.N. Flores¹²⁰, S. Foertsch⁷³, P. Foka¹⁰⁹, S. Fokin⁹⁰, E. Fragiaco⁶¹, U. Fuchs³⁵, N. Funicello³⁰, C. Furget⁸⁰, A. Furs⁶⁴, J.J. Gaardhøje⁹¹, M. Gagliardi²⁵, A.M. Gago¹¹³, A. Gal¹³⁸, C.D. Galvan¹²¹, P. Ganoti⁸⁶, C. Garabatos¹⁰⁹, J.R.A. Garcia⁴⁶, E. Garcia-Solis¹⁰, K. Garg¹¹⁶, C. Gargiulo³⁵, A. Garibli⁸⁹, K. Garner¹⁴⁵, P. Gasik¹⁰⁹, E.F. Gauger¹²⁰, A. Gautam¹²⁸, M.B. Gay Ducati⁷¹, M. Germain¹¹⁶, J. Ghosh¹¹¹, P. Ghosh¹⁴², S.K. Ghosh⁴, M. Giacalone²⁶, P. Gianotti⁵³, P. Giubellino^{109,60}, P. Giubileo²⁸, A.M.C. Glaenger¹³⁹, P. Glässel¹⁰⁶, V. Gonzalez¹⁴⁴, L.H. González-Trueba⁷², S. Gorbunov⁴⁰, L. Görlich¹¹⁹, S. Gotovac³⁶, V. Grabski⁷², L.K. Graczykowski¹⁴³, K.L. Graham¹¹², L. Greiner⁸¹, A. Grelli⁶³, C. Grigoras³⁵, V. Grigoriev⁹⁵, A. Grigoryan^{1,1}, S. Grigoryan^{76,1}, O.S. Groettvik²¹, F. Grosa⁶⁰, J.F. Grosse-Oetringhaus³⁵, R. Grosso¹⁰⁹, G.G. Guardiano¹²³, R. Guernane⁸⁰, M. Guilbaud¹¹⁶, M. Guittiere¹¹⁶, K. Gulbrandsen⁹¹, T. Gunji¹³⁴, A. Gupta¹⁰³, R. Gupta¹⁰³, I.B. Guzman⁴⁶, M.K. Habib¹⁰⁹, C. Hadjidakis⁷⁹, H. Hamagaki⁸⁴, G. Hamar¹⁴⁶,

M. Hamid⁷, R. Hannigan¹²⁰, M.R. Haque^{143,88}, A. Harlanderova¹⁰⁹, J.W. Harris¹⁴⁷, A. Harton¹⁰, J.A. Hasenbichler³⁵, H. Hassan⁹⁸, D. Hatzifotiadou⁵⁵, P. Hauer⁴⁴, L.B. Havener¹⁴⁷, S. Hayashi¹³⁴, S.T. Heckel¹⁰⁷, E. Hellbär⁶⁹, H. Helstrup³⁷, T. Herman³⁸, E.G. Hernandez⁴⁶, G. Herrera Corral⁹, F. Herrmann¹⁴⁵, K.F. Hetland³⁷, H. Hillemanns³⁵, C. Hills¹²⁹, B. Hippolyte¹³⁸, B. Hohlweger^{92,107}, J. Honermann¹⁴⁵, G.H. Hong¹⁴⁸, D. Horak³⁸, S. Hornung¹⁰⁹, R. Hosokawa¹⁵, P. Hristov³⁵, C. Huang⁷⁹, C. Hughes¹³², P. Huhn⁶⁹, T.J. Humanic⁹⁹, H. Hushnud¹¹¹, L.A. Husova¹⁴⁵, N. Hussain⁴³, D. Hutter⁴⁰, J.P. Iddon^{35,129}, R. Ilkaev¹¹⁰, H. Ilyas¹⁴, M. Inaba¹³⁵, G.M. Innocenti³⁵, M. Ippolitov⁹⁰, A. Isakov^{38,97}, M.S. Islam¹¹¹, M. Ivanov¹⁰⁹, V. Ivanov¹⁰⁰, V. Izucheev⁹³, B. Jacak⁸¹, N. Jacazio³⁵, P.M. Jacobs⁸¹, S. Jadlovská¹¹⁸, J. Jadlovsky¹¹⁸, S. Jaelani⁶³, C. Jahnke^{123,122}, M.J. Jakubowska¹⁴³, M.A. Janik¹⁴³, T. Janson⁷⁵, M. Jercic¹⁰¹, O. Jevons¹¹², F. Jonas^{98,145}, P.G. Jones¹¹², J.M. Jowett^{35,109}, J. Jung⁶⁹, M. Jung⁶⁹, A. Junique³⁵, A. Jusko¹¹², P. Kalinak⁶⁵, A. Kalweit³⁵, V. Kaplin⁹⁵, S. Kar⁷, A. Karasu Uysal⁷⁸, D. Karatovic¹⁰¹, O. Karavichev⁶⁴, T. Karavicheva⁶⁴, P. Karczmarczyk¹⁴³, E. Karpechev⁶⁴, A. Kazantsev⁹⁰, U. Keschull⁷⁵, R. Keidel⁴⁸, M. Keil³⁵, B. Ketzer⁴⁴, Z. Khabanova⁹², A.M. Khan⁷, S. Khan¹⁶, A. Khanzadeev¹⁰⁰, Y. Kharlov⁹³, A. Khatun¹⁶, A. Khuntia¹¹⁹, B. Kileng³⁷, B. Kim^{17,62}, D. Kim¹⁴⁸, D.J. Kim¹²⁷, E.J. Kim⁷⁴, J. Kim¹⁴⁸, J.S. Kim⁴², J. Kim¹⁰⁶, J. Kim¹⁴⁸, J. Kim⁷⁴, M. Kim¹⁰⁶, S. Kim¹⁸, T. Kim¹⁴⁸, S. Kirsch⁶⁹, I. Kisel⁴⁰, S. Kiselev⁹⁴, A. Kisiel¹⁴³, J.L. Klay⁶, J. Klein³⁵, S. Klein⁸¹, C. Klein-Bösing¹⁴⁵, M. Kleiner⁶⁹, T. Klemenz¹⁰⁷, A. Kluge³⁵, A.G. Knospe¹²⁶, C. Kobdaj¹¹⁷, M.K. Köhler¹⁰⁶, T. Kollegger¹⁰⁹, A. Kondratyev⁷⁶, N. Kondratyeva⁹⁵, E. Kondratyuk⁹³, J. König⁶⁹, S.A. Königstorfer¹⁰⁷, P.J. Konopka^{35,2}, G. Kornakov¹⁴³, S.D. Koryciak², L. Koska¹¹⁸, O. Kovalenko⁸⁷, V. Kovalenko¹¹⁴, M. Kowalski¹¹⁹, I. Králik⁶⁵, A. Kravčáková³⁹, L. Kreis¹⁰⁹, M. Krivda^{112,65}, F. Krizek⁹⁷, K. Krizkova Gajdosova³⁸, M. Kroesen¹⁰⁶, M. Krüger⁶⁹, E. Kryshen¹⁰⁰, M. Krzewicki⁴⁰, V. Kučera³⁵, C. Kuhn¹³⁸, P.G. Kuijper⁹², T. Kumaoka¹³⁵, L. Kumar¹⁰², S. Kundu^{35,88}, P. Kurashvili⁸⁷, A. Kurepin⁶⁴, A.B. Kurepin⁶⁴, A. Kuryakin¹¹⁰, S. Kushpil⁹⁷, J. Kvapil¹¹², M.J. Kweon⁶², J.Y. Kwon⁶², Y. Kwon¹⁴⁸, S.L. La Pointe⁴⁰, P. La Rocca²⁷, Y.S. Lai⁸¹, A. Lakrathok¹¹⁷, M. Lamanna³⁵, R. Langoy¹³¹, K. Lapidus³⁵, P. Larionov⁵³, E. Laudi³⁵, L. Lautner^{35,107}, R. Lavicka³⁸, T. Lazareva¹¹⁴, R. Lea^{141,24}, J. Lee¹³⁵, J. Leibrach⁴⁰, R.C. Lemmon⁹⁶, I. León Monzón¹²¹, E.D. Lesser¹⁹, M. Lettrich^{35,107}, P. Lévai¹⁴⁶, X. Li¹¹, X.L. Li⁷, J. Lien¹³¹, R. Lietava¹¹², B. Lim¹⁷, S.H. Lim¹⁷, V. Lindenstruth⁴⁰, A. Lindner⁴⁹, C. Lippmann¹⁰⁹, A. Liu¹⁹, J. Liu¹²⁹, I.M. Lofnes²¹, V. Loginov⁹⁵, C. Loizides⁹⁸, P. Loncar³⁶, J.A. Lopez¹⁰⁶, X. Lopez¹³⁶, E. López Torres⁸, J.R. Luhder¹⁴⁵, M. Lunardon²⁸, G. Luparello⁶¹, Y.G. Ma⁴¹, A. Maevskaya⁶⁴, M. Mager³⁵, T. Mahmoud⁴⁴, A. Maire¹³⁸, R.D. Majka^{147,1}, M. Malaev¹⁰⁰, Q.W. Malik²⁰, L. Malinina^{76,IV}, D. Mal'Kevich⁹⁴, N. Mallick⁵¹, P. Malzacher¹⁰⁹, G. Mandaglio^{33,57}, V. Manko⁹⁰, F. Manso¹³⁶, V. Manzari⁵⁴, Y. Mao⁷, J. Mareš⁶⁷, G.V. Margagliotti²⁴, A. Margotti⁵⁵, A. Marín¹⁰⁹, C. Markert¹²⁰, M. Marquard⁶⁹, N.A. Martin¹⁰⁶, P. Martinengo³⁵, J.L. Martinez¹²⁶, M.I. Martínez⁴⁶, G. Martínez García¹¹⁶, S. Masciocchi¹⁰⁹, M. Maserà²⁵, A. Masoni⁵⁶, L. Massacrier⁷⁹, A. Mastroserio^{140,54}, A.M. Mathis¹⁰⁷, O. Matonoha⁸², P.F.T. Matuoka¹²², A. Matyja¹¹⁹, C. Mayer¹¹⁹, A.L. Mazuecos³⁵, F. Mazzaschi²⁵, M. Mazzilli^{35,54}, M.A. Mazzoni⁵⁹, A.F. Mechler⁶⁹, F. Meddi²², Y. Melikyan⁶⁴, A. Menchaca-Rocha⁷², E. Meninno^{115,30}, A.S. Menon¹²⁶, M. Meres¹³, S. Mhlanga^{125,73}, Y. Miake¹³⁵, L. Micheletti²⁵, L.C. Migliorin¹³⁷, D.L. Mihaylov¹⁰⁷, K. Mikhaylov^{76,94}, A.N. Mishra^{146,70}, D. Miśkowiec¹⁰⁹, A. Modak⁴, A.P. Mohanty⁶³, B. Mohanty⁸⁸, M. Mohisin Khan¹⁶, Z. Moravcova⁹¹, C. Mordasini¹⁰⁷, D.A. Moreira De Godoy¹⁴⁵, L.A.P. Moreno⁴⁶, I. Morozov⁶⁴, A. Morsch³⁵, T. Mrnjavac³⁵, V. Muccifora⁵³, E. Mudnic³⁶, D. Mühlheim¹⁴⁵, S. Muhuri¹⁴², J.D. Mulligan⁸¹, A. Mulliri²³, M.G. Munhoz¹²², R.H. Munzer⁶⁹, H. Murakami¹³⁴, S. Murray¹²⁵, L. Musa³⁵, J. Musinsky⁶⁵, C.J. Myers¹²⁶, J.W. Myrcha¹⁴³, B. Naik⁵⁰, R. Nair⁸⁷, B.K. Nandi⁵⁰, R. Nania⁵⁵, E. Nappi⁵⁴, M.U. Naru¹⁴, A.F. Nassirpour⁸², C. Natrass¹³², A. Neagu²⁰, L. Nellen⁷⁰, S.V. Nesbo³⁷, G. Neskovic⁴⁰, D. Nesterov¹¹⁴, B.S. Nielsen⁹¹, S. Nikolaev⁹⁰, S. Nikulin⁹⁰, V. Nikulin¹⁰⁰, F. Noferini⁵⁵, S. Noh¹², P. Nomokonov⁷⁶, J. Norman¹²⁹, N. Novitzky¹³⁵, P. Nowakowski¹⁴³, A. Nyanin⁹⁰, J. Nystrand²¹, M. Ogino⁸⁴, A. Ohlson⁸², J. Oleniacz¹⁴³, A.C. Oliveira Da Silva¹³², M.H. Oliver¹⁴⁷, A. Onnerstad¹²⁷, C. Oppedisano⁶⁰, A. Ortiz Velasquez⁷⁰, T. Osako⁴⁷, A. Oskarsson⁸², J. Otwinowski¹¹⁹, K. Oyama⁸⁴, Y. Pachmayer¹⁰⁶, S. Padhan⁵⁰, D. Pagano¹⁴¹, G. Paic⁷⁰, A. Palasciano⁵⁴, J. Pan¹⁴⁴, S. Panebianco¹³⁹, P. Pareek¹⁴², J. Park⁶², J.E. Parkkila¹²⁷, S.P. Pathak¹²⁶, B. Paul²³, J. Pazzini¹⁴¹, H. Pei⁷, T. Peitzmann⁶³, X. Peng⁷, L.G. Pereira⁷¹, H. Pereira Da Costa¹³⁹, D. Peresunko⁹⁰, G.M. Perez⁸, S. Perrin¹³⁹, Y. Pestov⁵, V. Petráček³⁸, M. Petrovici⁴⁹, R.P. Pezzi⁷¹, S. Piano⁶¹, M. Pikna¹³, P. Pillot¹¹⁶, O. Pinazza^{55,35}, L. Pinsky¹²⁶, C. Pinto²⁷, S. Pisano⁵³, M. Płoskoń⁸¹, M. Planinic¹⁰¹, F. Pliquet⁶⁹, M.G. Poghosyan⁹⁸,

B. Polichtchouk⁹³, S. Politano³¹, N. Poljak¹⁰¹, A. Pop⁴⁹, S. Porteboeuf-Houssais¹³⁶, J. Porter⁸¹, V. Pozdniakov⁷⁶, S.K. Prasad⁴, R. Preghenella⁵⁵, F. Prino⁶⁰, C.A. Pruneau¹⁴⁴, I. Pshenichnov⁶⁴, M. Puccio³⁵, S. Qiu⁹², L. Quaglia²⁵, R.E. Quishpe¹²⁶, S. Ragoni¹¹², A. Rakotozafindrabe¹³⁹, L. Ramello³², F. Rami¹³⁸, S.A.R. Ramirez⁴⁶, A.G.T. Ramos³⁴, R. Raniwala¹⁰⁴, S. Raniwala¹⁰⁴, S.S. Räsänen⁴⁵, R. Rath⁵¹, I. Ravasenga⁹², K.F. Read^{98,132}, A.R. Redelbach⁴⁰, K. Redlich^{87,V}, A. Rehman²¹, P. Reichelt⁶⁹, F. Reidt³⁵, H.A. Reme-ness³⁷, R. Renfordt⁶⁹, Z. Rescakova³⁹, K. Reygers¹⁰⁶, A. Riabov¹⁰⁰, V. Riabov¹⁰⁰, T. Richert^{82,91}, M. Richter²⁰, W. Riegler³⁵, F. Riggi²⁷, C. Ristea⁶⁸, S.P. Rode⁵¹, M. Rodríguez Cahuantzi⁴⁶, K. Røed²⁰, R. Rogalev⁹³, E. Rogochaya⁷⁶, T.S. Rogoschinski⁶⁹, D. Rohr³⁵, D. Röhrich²¹, P.F. Rojas⁴⁶, P.S. Rokita¹⁴³, F. Ronchetti⁵³, A. Rosano^{33,57}, E.D. Rosas⁷⁰, A. Rossi⁵⁸, A. Rotondi²⁹, A. Roy⁵¹, P. Roy¹¹¹, N. Rubini²⁶, O.V. Rueda⁸², R. Rui²⁴, B. Rumyantsev⁷⁶, A. Rustamov⁸⁹, E. Ryabinkin⁹⁰, Y. Ryabov¹⁰⁰, A. Rybicki¹¹⁹, H. Rytönen¹²⁷, W. Rzesza¹⁴³, O.A.M. Saarimaki⁴⁵, R. Sadek¹¹⁶, S. Sadovsky⁹³, J. Saetre²¹, K. Šafařík³⁸, S.K. Saha¹⁴², S. Saha⁸⁸, B. Sahoo⁵⁰, P. Sahoo⁵⁰, R. Sahoo⁵¹, S. Sahoo⁶⁶, D. Sahu⁵¹, P.K. Sahu⁶⁶, J. Saini¹⁴², S. Sakai¹³⁵, S. Sambyal¹⁰³, V. Samsonov^{100,95,1}, D. Sarkar¹⁴⁴, N. Sarkar¹⁴², P. Sarma⁴³, V.M. Sarti¹⁰⁷, M.H.P. Sas¹⁴⁷, J. Schambach^{98,120}, H.S. Scheid⁶⁹, C. Schiaua⁴⁹, R. Schicker¹⁰⁶, A. Schmah¹⁰⁶, C. Schmidt¹⁰⁹, H.R. Schmidt¹⁰⁵, M.O. Schmidt¹⁰⁶, M. Schmidt¹⁰⁵, N.V. Schmidt^{98,69}, A.R. Schmier¹³², R. Schotter¹³⁸, J. Schukraft³⁵, Y. Schutz¹³⁸, K. Schwarz¹⁰⁹, K. Schweda¹⁰⁹, G. Scioli²⁶, E. Scomparin⁶⁰, J.E. Seger¹⁵, Y. Sekiguchi¹³⁴, D. Sekihata¹³⁴, I. Selyuzhenkov^{109,95}, S. Senyukov¹³⁸, J.J. Seo⁶², D. Serebryakov⁶⁴, L. Šerkšnytė¹⁰⁷, A. Sevcenco⁶⁸, T.J. Shaba⁷³, A. Shabanov⁶⁴, A. Shabetai¹¹⁶, R. Shahoyan³⁵, W. Shaikh¹¹¹, A. Shangaraev⁹³, A. Sharma¹⁰², H. Sharma¹¹⁹, M. Sharma¹⁰³, N. Sharma¹⁰², S. Sharma¹⁰³, O. Sheibani¹²⁶, K. Shigaki⁴⁷, M. Shimomura⁸⁵, S. Shirinkin⁹⁴, Q. Shou⁴¹, Y. Sibiriak⁹⁰, S. Siddhanta⁵⁶, T. Siemiarczuk⁸⁷, T.F. Silva¹²², D. Silvermyr⁸², G. Simonetti³⁵, B. Singh¹⁰⁷, R. Singh⁸⁸, R. Singh¹⁰³, R. Singh⁵¹, V.K. Singh¹⁴², V. Singhal¹⁴², T. Sinha¹¹¹, B. Sitar¹³, M. Sitta³², T.B. Skaali²⁰, G. Skorodumovs¹⁰⁶, M. Slupecki⁴⁵, N. Smirnov¹⁴⁷, R.J.M. Snellings⁶³, C. Soncco¹¹³, J. Song¹²⁶, A. Songmoonak¹¹⁷, F. Soramel²⁸, S. Sorensen¹³², I. Sputowska¹¹⁹, J. Stachel¹⁰⁶, I. Stan⁶⁸, P.J. Steffanic¹³², S.F. Stiefelmaier¹⁰⁶, D. Stocco¹¹⁶, M.M. Storetvedt³⁷, C.P. Stylianidis⁹², A.A.P. Suaide¹²², T. Sugitate⁴⁷, C. Suire⁷⁹, M. Suljic³⁵, R. Sultanov⁹⁴, M. Šumbera⁹⁷, V. Sumberia¹⁰³, S. Sumowidagdo⁵², S. Swain⁶⁶, A. Szabo¹³, I. Szarka¹³, U. Tabassam¹⁴, S.F. Taghavi¹⁰⁷, G. TAILLEPIED¹³⁶, J. Takahashi¹²³, G.J. Tambave²¹, S. Tang^{136,7}, Z. Tang¹³⁰, M. Tarhini¹¹⁶, M.G. Tarzila⁴⁹, A. Tauro³⁵, G. Tejada Muñoz⁴⁶, A. Telesca³⁵, L. Terlizzi²⁵, C. Terrevoli¹²⁶, G. Tersimonov³, S. Thakur¹⁴², D. Thomas¹²⁰, R. Tieulent¹³⁷, A. Tikhonov⁶⁴, A.R. Timmins¹²⁶, M. Tkacik¹¹⁸, A. Toia⁶⁹, N. Topilskaya⁶⁴, M. Toppi⁵³, F. Torres-Acosta¹⁹, S.R. Torres³⁸, A. Trifiró^{33,57}, S. Tripathy^{55,70}, T. Tripathy⁵⁰, S. Trogolo^{35,28}, G. Trombetta³⁴, V. Trubnikov³, W.H. Trzaska¹²⁷, T.P. Trzcinski¹⁴³, B.A. Trzeciak³⁸, A. Tumkin¹¹⁰, R. Turrisi⁵⁸, T.S. Tveter²⁰, K. Ullaland²¹, A. Uras¹³⁷, M. Urioni¹⁴¹, G.L. Usai²³, M. Vala³⁹, N. Valle²⁹, S. Vallero⁶⁰, N. van der Kolk⁶³, L.V.R. van Doremalen⁶³, M. van Leeuwen⁹², P. Vande Vyvre³⁵, D. Varga¹⁴⁶, Z. Varga¹⁴⁶, M. Varga-Kofarago¹⁴⁶, A. Vargas⁴⁶, M. Vasileiou⁸⁶, A. Vasiliev⁹⁰, O. Vázquez Doce¹⁰⁷, V. Vechernin¹¹⁴, E. Vercellin²⁵, S. Vergara Limón⁴⁶, L. Vermunt⁶³, R. Vértesi¹⁴⁶, M. Verweij⁶³, L. Vickovic³⁶, Z. Vilakazi¹³³, O. Villalobos Baillie¹¹², G. VINO⁵⁴, A. Vinogradov⁹⁰, T. Virgili³⁰, V. Vislavicius⁹¹, A. Vodopyanov⁷⁶, B. Volkel³⁵, M.A. Völkl¹⁰⁵, K. Voloshin⁹⁴, S.A. Voloshin¹⁴⁴, G. Volpe³⁴, B. von Haller³⁵, I. Vorobyev¹⁰⁷, D. Voscek¹¹⁸, J. Vrláková³⁹, B. Wagner²¹, M. Weber¹¹⁵, A. Wegrzynek³⁵, S.C. Wenzel³⁵, J.P. Wessels¹⁴⁵, J. Wiechula⁶⁹, J. Wikne²⁰, G. Wilk⁸⁷, J. Wilkinson¹⁰⁹, G.A. Willems¹⁴⁵, E. Willsher¹¹², B. Windelband¹⁰⁶, M. Winn¹³⁹, W.E. Witt¹³², J.R. Wright¹²⁰, Y. Wu¹³⁰, R. Xu⁷, S. Yalcin⁷⁸, Y. Yamaguchi⁴⁷, K. Yamakawa⁴⁷, S. Yang²¹, S. Yano^{47,139}, Z. Yin⁷, H. Yokoyama⁶³, I.-K. Yoo¹⁷, J.H. Yoon⁶², S. Yuan²¹, A. Yuncu¹⁰⁶, V. Zaccolo²⁴, A. Zaman¹⁴, C. Zampolli³⁵, H.J.C. Zanoli⁶³, N. Zardoshti³⁵, A. Zarochentsev¹¹⁴, P. Závada⁶⁷, N. Zaviyalov¹¹⁰, H. Zbroszczyk¹⁴³, M. Zhalov¹⁰⁰, S. Zhang⁴¹, X. Zhang⁷, Y. Zhang¹³⁰, V. Zhrebchevskii¹¹⁴, Y. Zhi¹¹, D. Zhou⁷, Y. Zhou⁹¹, J. Zhu^{7,109}, Y. Zhu⁷, A. Zichichi²⁶, G. Zinovjev³, N. Zurlo¹⁴¹,

¹ A.I. Alikhanyan National Science Laboratory (Yerevan Physics Institute) Foundation, Yerevan, Armenia

² AGH University of Science and Technology, Cracow, Poland

³ Bogolyubov Institute for Theoretical Physics, National Academy of Sciences of Ukraine, Kiev, Ukraine

⁴ Bose Institute, Department of Physics and Centre for Astroparticle Physics and Space Science (CAPSS), Kolkata, India

⁵ Budker Institute for Nuclear Physics, Novosibirsk, Russia

⁶ California Polytechnic State University, San Luis Obispo, CA, United States

⁷ Central China Normal University, Wuhan, China

⁸ Centro de Aplicaciones Tecnológicas y Desarrollo Nuclear (CEADEN), Havana, Cuba

⁹ Centro de Investigación y de Estudios Avanzados (CINVESTAV), Mexico City and Mérida, Mexico

¹⁰ Chicago State University, Chicago, IL, United States

- 11 China Institute of Atomic Energy, Beijing, China
 12 Chungbuk National University, Cheongju, Republic of Korea
 13 Comenius University Bratislava, Faculty of Mathematics, Physics and Informatics, Bratislava, Slovakia
 14 COMSATS University Islamabad, Islamabad, Pakistan
 15 Creighton University, Omaha, NE, United States
 16 Department of Physics, Aligarh Muslim University, Aligarh, India
 17 Department of Physics, Pusan National University, Pusan, Republic of Korea
 18 Department of Physics, Sejong University, Seoul, Republic of Korea
 19 Department of Physics, University of California, Berkeley, CA, United States
 20 Department of Physics, University of Oslo, Oslo, Norway
 21 Department of Physics and Technology, University of Bergen, Bergen, Norway
 22 Dipartimento di Fisica dell'Università 'La Sapienza' and Sezione INFN, Rome, Italy
 23 Dipartimento di Fisica dell'Università and Sezione INFN, Cagliari, Italy
 24 Dipartimento di Fisica dell'Università and Sezione INFN, Trieste, Italy
 25 Dipartimento di Fisica dell'Università and Sezione INFN, Turin, Italy
 26 Dipartimento di Fisica e Astronomia dell'Università and Sezione INFN, Bologna, Italy
 27 Dipartimento di Fisica e Astronomia dell'Università and Sezione INFN, Catania, Italy
 28 Dipartimento di Fisica e Astronomia dell'Università and Sezione INFN, Padova, Italy
 29 Dipartimento di Fisica e Nucleare e Teorica, Università di Pavia and Sezione INFN, Pavia, Italy
 30 Dipartimento di Fisica 'E.R. Caianiello' dell'Università and Gruppo Collegato INFN, Salerno, Italy
 31 Dipartimento DISAT del Politecnico and Sezione INFN, Turin, Italy
 32 Dipartimento di Scienze e Innovazione Tecnologica dell'Università del Piemonte Orientale and INFN Sezione di Torino, Alessandria, Italy
 33 Dipartimento di Scienze MIFT, Università di Messina, Messina, Italy
 34 Dipartimento Interateneo di Fisica 'M. Merlin' and Sezione INFN, Bari, Italy
 35 European Organization for Nuclear Research (CERN), Geneva, Switzerland
 36 Faculty of Electrical Engineering, Mechanical Engineering and Naval Architecture, University of Split, Split, Croatia
 37 Faculty of Engineering and Science, Western Norway University of Applied Sciences, Bergen, Norway
 38 Faculty of Nuclear Sciences and Physical Engineering, Czech Technical University in Prague, Prague, Czech Republic
 39 Faculty of Science, P.J. Šafárik University, Košice, Slovakia
 40 Frankfurt Institute for Advanced Studies, Johann Wolfgang Goethe-Universität Frankfurt, Frankfurt, Germany
 41 Fudan University, Shanghai, China
 42 Gangneung-Wonju National University, Gangneung, Republic of Korea
 43 Gauhati University, Department of Physics, Guwahati, India
 44 Helmholtz-Institut für Strahlen- und Kernphysik, Rheinische Friedrich-Wilhelms-Universität Bonn, Bonn, Germany
 45 Helsinki Institute of Physics (HIP), Helsinki, Finland
 46 High Energy Physics Group, Universidad Autónoma de Puebla, Puebla, Mexico
 47 Hiroshima University, Hiroshima, Japan
 48 Hochschule Worms, Zentrum für Technologietransfer und Telekommunikation (ZTT), Worms, Germany
 49 Horia Hulubei National Institute of Physics and Nuclear Engineering, Bucharest, Romania
 50 Indian Institute of Technology Bombay (IIT), Mumbai, India
 51 Indian Institute of Technology Indore, Indore, India
 52 Indonesian Institute of Sciences, Jakarta, Indonesia
 53 INFN, Laboratori Nazionali di Frascati, Frascati, Italy
 54 INFN, Sezione di Bari, Bari, Italy
 55 INFN, Sezione di Bologna, Bologna, Italy
 56 INFN, Sezione di Cagliari, Cagliari, Italy
 57 INFN, Sezione di Catania, Catania, Italy
 58 INFN, Sezione di Padova, Padova, Italy
 59 INFN, Sezione di Roma, Rome, Italy
 60 INFN, Sezione di Torino, Turin, Italy
 61 INFN, Sezione di Trieste, Trieste, Italy
 62 Inha University, Incheon, Republic of Korea
 63 Institute for Gravitational and Subatomic Physics (GRASP), Utrecht University/Nikhef, Utrecht, Netherlands
 64 Institute for Nuclear Research, Academy of Sciences, Moscow, Russia
 65 Institute of Experimental Physics, Slovak Academy of Sciences, Košice, Slovakia
 66 Institute of Physics, Homi Bhabha National Institute, Bhubaneswar, India
 67 Institute of Physics of the Czech Academy of Sciences, Prague, Czech Republic
 68 Institute of Space Science (ISS), Bucharest, Romania
 69 Institut für Kernphysik, Johann Wolfgang Goethe-Universität Frankfurt, Frankfurt, Germany
 70 Instituto de Ciencias Nucleares, Universidad Nacional Autónoma de México, Mexico City, Mexico
 71 Instituto de Física, Universidade Federal do Rio Grande do Sul (UFRGS), Porto Alegre, Brazil
 72 Instituto de Física, Universidad Nacional Autónoma de México, Mexico City, Mexico
 73 iThemba LABS, National Research Foundation, Somerset West, South Africa
 74 Jeonbuk National University, Jeonju, Republic of Korea
 75 Johann-Wolfgang-Goethe Universität Frankfurt Institut für Informatik, Fachbereich Informatik und Mathematik, Frankfurt, Germany
 76 Joint Institute for Nuclear Research (JINR), Dubna, Russia
 77 Korea Institute of Science and Technology Information, Daejeon, Republic of Korea
 78 KTO Karatay University, Konya, Turkey
 79 Laboratoire de Physique des 2 Infinis, Irène Joliot-Curie, Orsay, France
 80 Laboratoire de Physique Subatomique et de Cosmologie, Université Grenoble-Alpes, CNRS-IN2P3, Grenoble, France
 81 Lawrence Berkeley National Laboratory, Berkeley, CA, United States
 82 Lund University Department of Physics, Division of Particle Physics, Lund, Sweden
 83 Moscow Institute for Physics and Technology, Moscow, Russia
 84 Nagasaki Institute of Applied Science, Nagasaki, Japan
 85 Nara Women's University (NWU), Nara, Japan
 86 National and Kapodistrian University of Athens, School of Science, Department of Physics, Athens, Greece
 87 National Centre for Nuclear Research, Warsaw, Poland
 88 National Institute of Science Education and Research, Homi Bhabha National Institute, Jatni, India
 89 National Nuclear Research Center, Baku, Azerbaijan
 90 National Research Centre Kurchatov Institute, Moscow, Russia

- 91 Niels Bohr Institute, University of Copenhagen, Copenhagen, Denmark
 92 Nikhef, National institute for subatomic physics, Amsterdam, Netherlands
 93 NRC Kurchatov Institute IHEP, Protvino, Russia
 94 NRC «Kurchatov» Institute – ITEP, Moscow, Russia
 95 NRNU Moscow Engineering Physics Institute, Moscow, Russia
 96 Nuclear Physics Group, STFC Daresbury Laboratory, Daresbury, United Kingdom
 97 Nuclear Physics Institute of the Czech Academy of Sciences, Řež u Prahy, Czech Republic
 98 Oak Ridge National Laboratory, Oak Ridge, TN, United States
 99 Ohio State University, Columbus, OH, United States
 100 Petersburg Nuclear Physics Institute, Gatchina, Russia
 101 Physics department, Faculty of science, University of Zagreb, Zagreb, Croatia
 102 Physics Department, Panjab University, Chandigarh, India
 103 Physics Department, University of Jammu, Jammu, India
 104 Physics Department, University of Rajasthan, Jaipur, India
 105 Physikalisches Institut, Eberhard-Karls-Universität Tübingen, Tübingen, Germany
 106 Physikalisches Institut, Ruprecht-Karls-Universität Heidelberg, Heidelberg, Germany
 107 Physik Department, Technische Universität München, Munich, Germany
 108 Politecnico di Bari and Sezione INFN, Bari, Italy
 109 Research Division and ExtreMe Matter Institute EMMI, GSI Helmholtzzentrum für Schwerionenforschung GmbH, Darmstadt, Germany
 110 Russian Federal Nuclear Center (VNIIEF), Sarov, Russia
 111 Saha Institute of Nuclear Physics, Homi Bhabha National Institute, Kolkata, India
 112 School of Physics and Astronomy, University of Birmingham, Birmingham, United Kingdom
 113 Sección Física, Departamento de Ciencias, Pontificia Universidad Católica del Perú, Lima, Peru
 114 St. Petersburg State University, St. Petersburg, Russia
 115 Stefan Meyer Institut für Subatomare Physik (SMI), Vienna, Austria
 116 SUBATECH, IMT Atlantique, Université de Nantes, CNRS-IN2P3, Nantes, France
 117 Suranaree University of Technology, Nakhon Ratchasima, Thailand
 118 Technical University of Košice, Košice, Slovakia
 119 The Henryk Niewodniczanski Institute of Nuclear Physics, Polish Academy of Sciences, Cracow, Poland
 120 The University of Texas at Austin, Austin, TX, United States
 121 Universidad Autónoma de Sinaloa, Culiacán, Mexico
 122 Universidade de São Paulo (USP), São Paulo, Brazil
 123 Universidade Estadual de Campinas (UNICAMP), Campinas, Brazil
 124 Universidade Federal do ABC, Santo Andre, Brazil
 125 University of Cape Town, Cape Town, South Africa
 126 University of Houston, Houston, TX, United States
 127 University of Jyväskylä, Jyväskylä, Finland
 128 University of Kansas, Lawrence, KS, United States
 129 University of Liverpool, Liverpool, United Kingdom
 130 University of Science and Technology of China, Hefei, China
 131 University of South-Eastern Norway, Tonsberg, Norway
 132 University of Tennessee, Knoxville, TN, United States
 133 University of the Witwatersrand, Johannesburg, South Africa
 134 University of Tokyo, Tokyo, Japan
 135 University of Tsukuba, Tsukuba, Japan
 136 Université Clermont Auvergne, CNRS/IN2P3, LPC, Clermont-Ferrand, France
 137 Université de Lyon, CNRS/IN2P3, Institut de Physique des 2 Infinis de Lyon, Lyon, France
 138 Université de Strasbourg, CNRS, IPHC UMR 7178, F-67000, Strasbourg, France
 139 Université Paris-Saclay Centre d'Etudes de Saclay (CEA), IRFU, Département de Physique Nucléaire (DPhN), Saclay, France
 140 Università degli Studi di Foggia, Foggia, Italy
 141 Università di Brescia and Sezione INFN, Brescia, Italy
 142 Variable Energy Cyclotron Centre, Homi Bhabha National Institute, Kolkata, India
 143 Warsaw University of Technology, Warsaw, Poland
 144 Wayne State University, Detroit, MI, United States
 145 Westfälische Wilhelms-Universität Münster, Institut für Kernphysik, Münster, Germany
 146 Wigner Research Centre for Physics, Budapest, Hungary
 147 Yale University, New Haven, CT, United States
 148 Yonsei University, Seoul, Republic of Korea

^I Deceased.

^{II} Also at: Italian National Agency for New Technologies, Energy and Sustainable Economic Development (ENEA), Bologna, Italy.

^{III} Also at: Dipartimento DET del Politecnico di Torino, Turin, Italy.

^{IV} Also at: M.V. Lomonosov Moscow State University, D.V. Skobel'syn Institute of Nuclear, Physics, Moscow, Russia.

^V Also at: Institute of Theoretical Physics, University of Wrocław, Poland.